Technical Report No. 32-495

Telemetry and Command Techniques for Planetary Spacecraft

J. C. Springett

R. B. Harker, *Chief*
Spacecraft Telemetry and Command Section

JET PROPULSION LABORATORY
CALIFORNIA INSTITUTE OF TECHNOLOGY
PASADENA, CALIFORNIA

January 15, 1965

I

Copyright © 1965
Jet Propulsion Laboratory
California Institute of Technology

Prepared Under Contract No. NAS 7-100
National Aeronautics & Space Administration

CONTENTS

TABLES

FIGURES

FIGURES (Cont'd)

PREFACE

The material in this Report also appears as the chapter "Telemetry and Command Techniques for Planetary Spacecraft" in the book *Advances in Communication Systems,* edited by A. V. Balakrishnan and published in December 1964 by the Academic Press, Inc.

ABSTRACT

15406

Communication with planetary spacecraft, where system constraints allow data rates of only a few bits per second, requires that the method used to obtain synchronization does not significantly degrade the theoretical performance of the link. A method is presented whereby bit and word synchronization can be achieved without the use of zero-crossing detectors and without the inclusion of sync words within the data format. The modulation and detection system makes use of maximal-length linear shift-register codes in conjunction with phase-lock techniques to achieve unambiguous code synchronization from which bit sync, word sync, and coherent demodulation signals can be obtained. In addition, the data bits and the sync code are combined mod-2, thereby realizing an optimum system from the standpoint of providing all of the available transmitter sideband power to the data signal, as well as the synchronization signal.

I. THE PLANETARY MISSIONS

The primary long-range objective of the planetary program of the National Aeronautics and Space Administration (NASA) and the Jet Propulsion Laboratory (JPL) is the development of unmanned interplanetary spacecraft and technology for the purpose of gathering fundamental scientific knowledge concerning the planetary and interplanetary environments. High on the list of priorities is the search for life forms, if any, on the nearby planets, Mars, Venus, Mercury, and Jupiter. In addition, scientific experiments will explore such interplanetary phenomena as solar plasma, micrometeorite densities, and magnetic fields, and such planetary characteristics as atmospheric and surface composition.

A secondary long-range objective of the JPL planetary program is the advancement of deep-space technology and the collection of data that will contribute to the eventual exploration of space and the planets by manned vehicles.

The first United States spacecraft to partially fulfill a limited number of these objectives was the *Mariner 2*, which achieved a successful rendezvous (flyby trajectory) with the planet Venus on December 14, 1962.

In further fulfillment of these objectives, it is planned by 1970 to have rather completely demonstrated that spacecraft are capable of (1) being put into orbit around Mars and Venus, and (2) landing on the surface of these planets. There will also be efforts to extend this capability toward the planets Mercury and Jupiter, and to send probes out of the plane of the ecliptic and in toward the Sun.

II. FUNDAMENTALS OF COMMUNICATION LINKS

A. Requirements

The objectives of the planetary program place a number of important requirements upon the communications system between the spacecraft and the Earth. These requirements fall into three main categories: tracking, telemetry, and command.

1. Tracking

Tracking is required in order to determine the trajectory of the spacecraft accurately after its separation from the boost or launch vehicle. The tracking information consists of (1) vehicle velocity, measured through doppler frequency shift, (2) angular position, and (3) range.

The doppler measurement can be made through either one-way or two-way techniques. For one-way doppler measurements, the "apparent" frequency shift of the spacecraft transmitter is determined. The word "apparent" is used since the radio frequency (RF) carrier frequency is generally not known with sufficient resolution (owing to temperature drifts), resulting in a one-way doppler measurement of low accuracy. However, with a two-way doppler system, a very stable RF carrier is transmitted to the spacecraft, coherently detected, filtered, translated in frequency, and retransmitted to the Earth. In order to achieve the required accuracy, the two-way doppler system must maintain complete phase coherence throughout, and as a result, the spacecraft receiver is of the automatic phase-control type (phase-locked loop), of which more will be said in subsequent sections.

The angular position of the spacecraft is determined with respect to the coordinates of the tracking stations by measuring the apparent angle of arrival of the spacecraft transmitter signal. In order to accomplish this, simultaneous-lobing antennas are employed in conjunction with coherent receivers.

Finally, range may be measured through an extension of the two-way doppler system. The simplest method is to modulate the carrier with an audio frequency and compare its transmitted and received phases. The disadvantages of using a single tone are that (1) it is impossible to transmit and detect a tone of sufficiently low frequency to circumvent range ambiguity, and (2) the resolution of the phase measurement is generally poor. To avoid these problems, the tone may be replaced by a pseudorandom periodic binary sequence whose period is greater than the round-trip propagation time for the greatest range to be measured. The techniques for acquiring binary sequences similar to those used for ranging will be presented in Section IV.

2. Telemetry

The telemetry link is the voice of the spacecraft and provides two basic types of information: performance and experimental. The performance measurements pertain to spacecraft operating conditions and consist of temperature, pressure, voltage and current, subsystems monitors, events, etc. Experimental measurements are related to the scientific objectives of the mission, such as the investigation of solar plasma, magnetic fields, and micrometeorites, and information from scan systems, including television.

Because of the large number of measurements to be made, it is necessary to time-multiplex them in accordance with some priority, and also to provide more than one mode of operation (for example, Mode I, all performance data; Mode II, mixed performance and experimental; and Mode III, all experimental). In addition, the information rate that the telemetry link can support is a function of time or spacecraft range.

3. Command

The command link is required to supply information needed by the various spacecraft subsystems after launch. Many commands are necessary to the routine operation and control of spacecraft functions; some are provided for changing the mission emphasis if unusual or unexpected conditions are encountered, while others are required to correct erratic operations or to partially salvage the mission if a spacecraft failure occurs. Command information varies in complexity from simple "on–off" operations to trajectory-correction factors (based on tracking) for maneuvers. Usually, all of the commands will fall into two classes, (1) the discrete command for switching functions, which requires only an address for identification and execution, and (2) the quantitative command, which requires a magnitude in addition to the address.

B. Limitations

Four major limitations become evident in the design of the communication system to meet the requirements discussed above: (1) the maximum available transmitter power, (2) the size and characteristics of the transmitting and receiving antennas, (3) the free-space loss, and (4) the noise temperature of the receiving system.

1. Transmitter and Antenna Systems

Referring to the spacecraft transmitting system, it is generally most meaningful to think in terms of the gain–power product required for the mission. Once the gain–power product has been determined, trade-offs can be made between the size of the antenna (assumed to be parabolic) and the transmitter power. The upper bound on transmitter power is dictated by the weight and physical size of the transmitter, plus the amount of primary power available, while the antenna size is dependent primarily upon weight and the physical constraints of the spacecraft and the launch vehicle. At first glance, it might seem best to use low transmitter powers and large (perhaps erectable) antennas to achieve a required gain–power product; however, large parabolic antennas (over 8 ft in diameter) have 3-db beam angles of 3 deg or less and must be very precisely pointed. As a result, utilization of large antennas generally requires that some form of angle-tracking signal be transmitted from the Earth to obtain the necessary pointing accuracy.

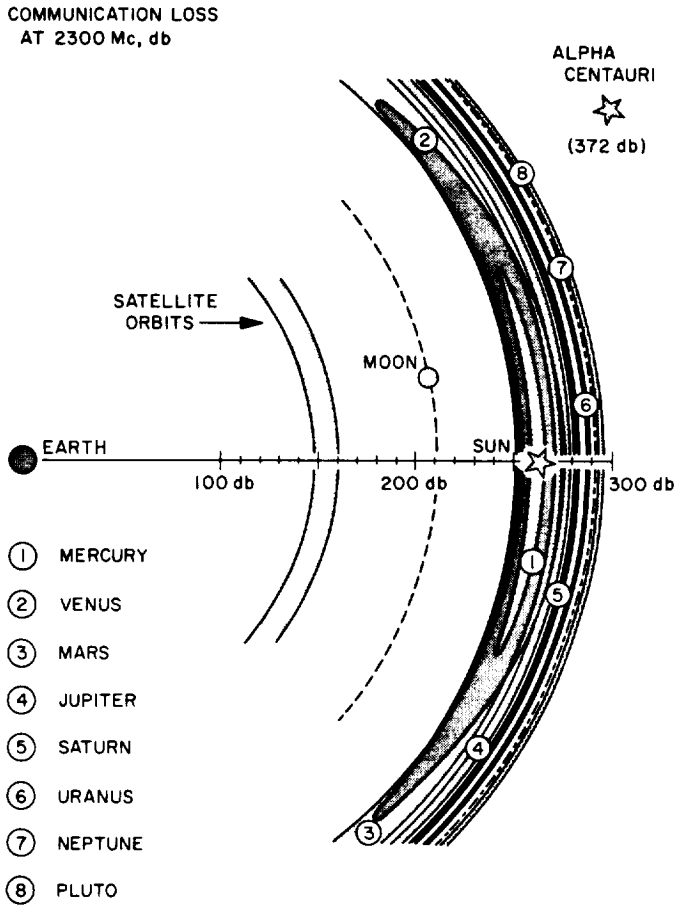

Fig. 1. The solar system as seen by a communications engineer from a nonrotating Earth

2. Free-Space Loss

Free-space loss is the path attenuation between two isotropic antennas and is given by

$$L_s(\text{db}) = 32.45 + 20\log_{10}(f) + 20\log_{10}(R) \qquad (1)$$

where f is the transmitting frequency in megacycles per second and R is the path distance in kilometers. Figure 1 shows a diagram of the solar system as seen from a nonrotating Earth, with the distance from the Earth plotted in terms of L_s at a frequency of 2,300 Mc (Ref. 1). As can be seen, the planets range between 250 and 295 db as compared with 155 db for most Earth satellites.

When both the transmitting and the receiving antennas are parabolic, it is advantageous to choose the transmitting frequency as high as possible (within the constraints of frequency allocations, state-of-the-art mechanization, and atmospheric absorption) in order to maximize the received signal power. Since the gain of a parabolic receiving antenna is given by

$$G(\text{db}) = 43.27 + 20\log_{10}(f) + 20\log_{10}(D) \qquad (2)$$

where f is the frequency in megacycles per second and D is the antenna diameter in meters, then the advantage as a function of a higher frequency over a lower frequency is the increase in the transmitting and receiving antenna gains minus the increase in space loss, or simply the increase in either of the antenna gains.

3. Noise Temperature of the Receiving System

The noise temperature of the receiving system (assuming the antenna to be pointing along the zenith) depends primarily upon the internal thermal noise of the receiver, the noise temperature of the antenna feed, and the external noise introduced through the antenna sidelobes.

Receivers with vacuum tube amplifiers have equivalent noise temperatures of approximately 2000°K, while parametric amplifiers have noise temperatures of about 100°K, and masers, between 5 and 20°K. The noise temperature of the antenna and feed system is dependent upon a number of factors, such as frequency, antenna size and structure, feed-line loss, etc., and for large, well engineered antenna systems, will generally fall between 15 and 25°K. The total noise temperature of the system will then fall between 20 and 45°K for a maser receiver. Obviously these noise temperatures must be increased somewhat when the antenna is pointed closer to the horizon or at other noise sources, such as the planets.

Table 1 summarizes typical characteristics of transmitting and receiving systems for the JPL Deep Space Instrumentation Facility (DSIF) and for spacecraft of the *Mariner* and *Voyager* classes.

C. *The Generalized Communications System*

Figure 2 shows simplified block diagrams of the spacecraft and ground communications systems. The data-handling system functions to condition and time-multiplex the performance and experimental telemetry data in accordance with priority and operational modes. Both bit- and word-timing signals are supplied to the data-handling system by the telemetry modulator.

The telemetry modulator generates all bit- and word-synchronizing signals and combines them with the processed telemetry data for subsequent modulation of the spacecraft transmitter. Also modulating the transmitter is the ranging code derived from the Earth-to-spacecraft link and processed in the ranging detector–decoder.

The output of the transponder receiver contains command and sync information which is demodulated and

Table 1. Characteristics of transmitting and receiving systems

<table>
<tr><th>Year</th><th>Transmitter power, w</th><th>Transmitting antenna diameter, ft</th><th>Transmitting frequency, Mc</th><th>Receiving antenna diameter, ft</th><th>System temperature, °K</th></tr>
<tr><td></td><td colspan="5">Spacecraft to Earth</td></tr>
<tr><td>1962
1963</td><td>3</td><td rowspan="2">4</td><td>960</td><td rowspan="2">85</td><td rowspan="2">220
or
40</td></tr>
<tr><td>1964
1965</td><td rowspan="2">10</td><td rowspan="3">2295</td></tr>
<tr><td>1966</td><td rowspan="2">85
to
210</td><td>30</td></tr>
<tr><td>1967
1968
1969</td><td>25
to
100</td><td>8
to
15</td><td>25</td></tr>
<tr><td></td><td colspan="5">Earth to spacecraft</td></tr>
<tr><td>1962
1963</td><td>10 kw</td><td rowspan="4">85</td><td>890</td><td rowspan="2">omni</td><td>3200</td></tr>
<tr><td>1964
1965</td><td rowspan="3">10 kw
or
100 kw</td><td rowspan="3">2115</td><td rowspan="2">1800</td></tr>
<tr><td>1966
1967</td><td rowspan="2">omni
or
8
to
15</td></tr>
<tr><td>1968
1969</td><td>730</td></tr>
</table>

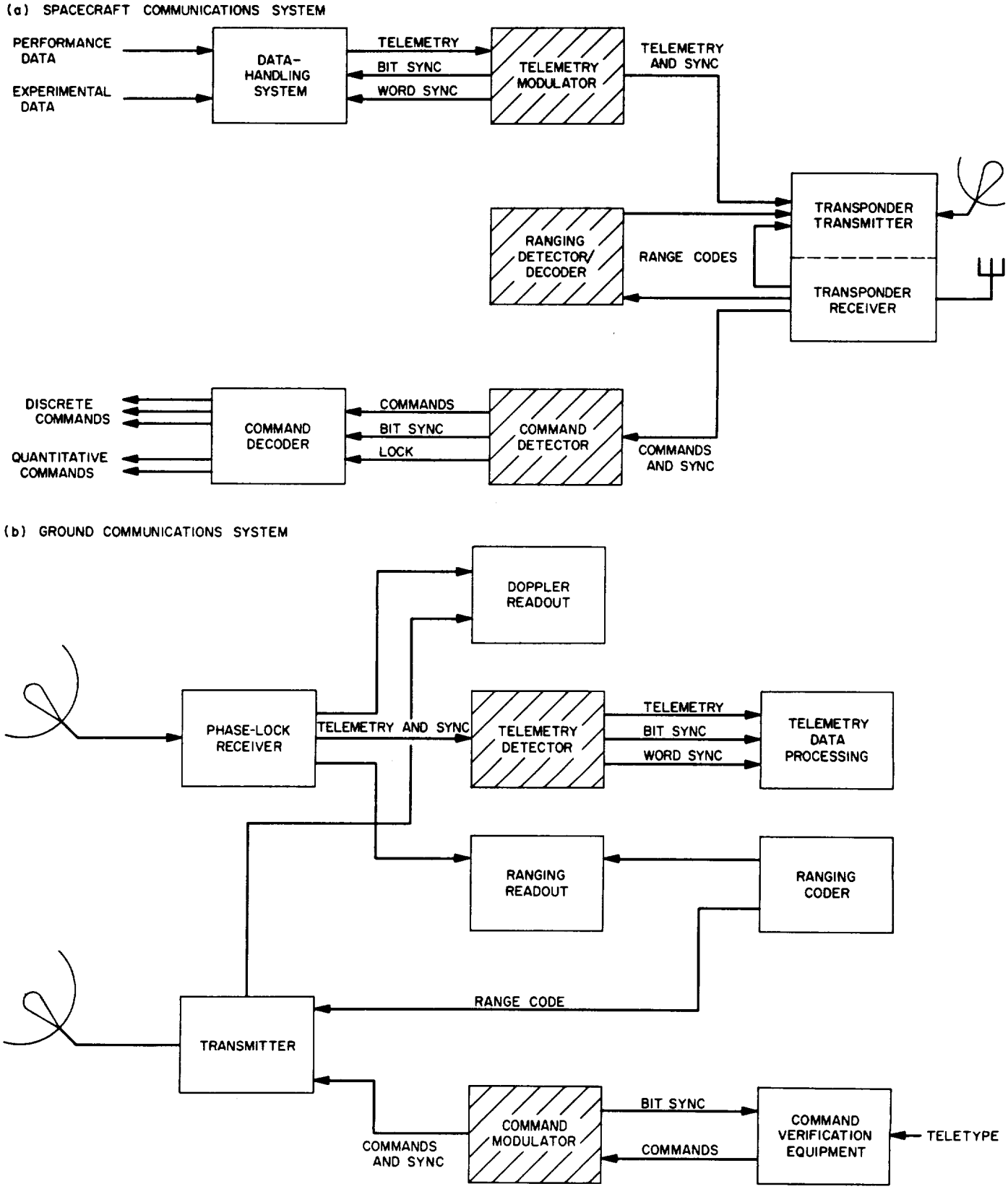

Fig. 2. Spacecraft and ground communications subsystems

detected in the spacecraft command detector. The command detector supplies to the decoder, which follows it, the demodulated and detected command bits together with bit sync, plus a lock signal to inform the decoder when valid command signals are present. The decoder in turn serves to recognize which command has been received and to initiate the proper action.

The output of the ground receiver contains doppler, ranging, and telemetry information. The telemetry detector demodulates and detects the telemetry signal and provides the telemetry data processing system with the telemetry data bits, bit sync, and word sync.

The ranging readout provides a comparison between transmitted and received range codes, wherein two-way range is determined as a function of code phase or displacement.

Commands to the spacecraft are checked and processed by the command verification equipment, with bit synchronization being supplied by the command modulator. The command modulator generates synchronization signals and combines them with the command information for subsequent modulation of the transmitter.

It should be pointed out that modulation for both the spacecraft and the ground transmitter is accomplished with relatively low modulation indices, so that the RF carriers are not completely suppressed.

The remaining sections will be devoted primarily to the theory of the techniques that are currently being exploited for implementation of the modulation, detection, and synchronization portions (shaded blocks, Fig. 2) of the telemetry and command links.

The general properties of the RF systems are fixed, owing to standard DSIF and spacecraft transponder mechanization, and as a result, the telemetry and command systems must be designed to operate within DSIF and transponder constraints and limitations.

III. TELEMETRY AND COMMAND SYSTEM PHILOSOPHY

A. Comparison of Telemetry and Command Links

A number of significant similarities exist between the telemetry and command links, thereby implying that their modulation and detection systems should embody the same basic techniques. First, both links employ automatic phase control (phase-locked loop) receivers with nearly identical characteristics, the only major difference being their noise temperatures. Secondly, because of the need for efficiency, simplicity, and reliability, each system is digital, with information being conveyed over a single pulse-code modulated (PCM) channel. Finally, as will be seen shortly, the maximum data rates that can be employed are very low in comparison with the data rates obtainable from missiles and satellites; the command system operates at a few bits per second (bps), and the telemetry link, at not more than a few hundred bps.

The only major difference between the telemetry and command links is the required bit error rate, or bit error probability, P_e^b. Acceptable telemetry data can be obtained for bit error rates ranging between 1×10^{-2} errors per bit and 1×10^{-3} errors per bit, while the command system, which cannot permit command errors, requires bit error rates of 1×10^{-5} errors per bit or less.

B. Data Rate Capabilities

The normalized received signal-to-noise ratio (SNR) for either the telemetry or the command link is given by

$$S/(N/B) = P_t + G_T + G_R - \Phi_K - L_s - L_m - \sum L_T \quad (3)$$

where $S/(N/B)$ = normalized received SNR, db-cps

P_s = sideband transmitter power, dbm

G_T = transmitting antenna gain, db

G_R = receiving antenna gain, db

Φ_K = receiving system noise spectral density, dbm/cps

L_S = space loss, db

L_m = miscellaneous loss, db

L_T = system negative tolerances, db

Referring to the current state-of-the-art for the DSIF and to a typical spacecraft transmission system, the received telemetry SNR for a Mars mission is calculated from Eq. (3) with the following parameters:

P_s = 41 dbm (assuming power divided equally between carrier and sidebands)

G_T = 26.4 db (4-ft parabolic)

G_R = 51.0 db (85-ft parabolic)

Φ_K = − 186.6 dbm/cps (40°K)

L_S = 266.5 db (2.2×10^8 km; 2,300 Mc)

L_m = 2.0 db

$\sum L_T$ = 6.0 db

Substituting in Eq. (3), we obtain

$$S/(N/B) = 30.5 \text{ db-cps}$$

Before the data rate can be determined, a type of PCM modulation and detection must be chosen. Efficiency, i.e., minimizing the required signal energy per bit for a fixed bit error probability, is most important, since the system is essentially power-limited rather than bandwidth-limited; therefore, the proven optimum choice is a biorthogonal channel employing coherent demodulation and matched-filter (MF) detection (Ref. 2, 3). The present discussion will be concerned only with the techniques involved for the mechanization of the uncoded channel [bit or symbol detection, often referred to as coherent phase-shift-keying (PSK)] as opposed to the coded (word detection) channel. The relationship between the bit error probability, the received signal energy per bit, E (in joules), and the noise power per unit bandwidth, N/B (watts/cps), is

$$P_e^b = 1/2 \left[1 - erf \sqrt{E/(N/B)}\right] \quad (4)$$

where *erf* denotes the error function. Figure 3 shows a plot of Eq. (4).

Since the signal energy is equal to the product of the signal power and the bit period T (in seconds), then, in logarithmic notation,

$$E/(N/B) = ST/(N/B) = S/(N/B) + T \quad (5)$$

or

$$T = E/(N/B) - S/(N/B) \quad (6)$$

Through the arbitrary choice of $P_e^b = 1 \times 10^{-3}$, Eq. (4) yields $E/(N/B) = 6.8$ db, and substituting this, together with the previously obtained $S/(N/B) = 30.5$ db-cps into Eq. (6), the data rate, $R = 1/T$, for the telemetry link is 234 bps.

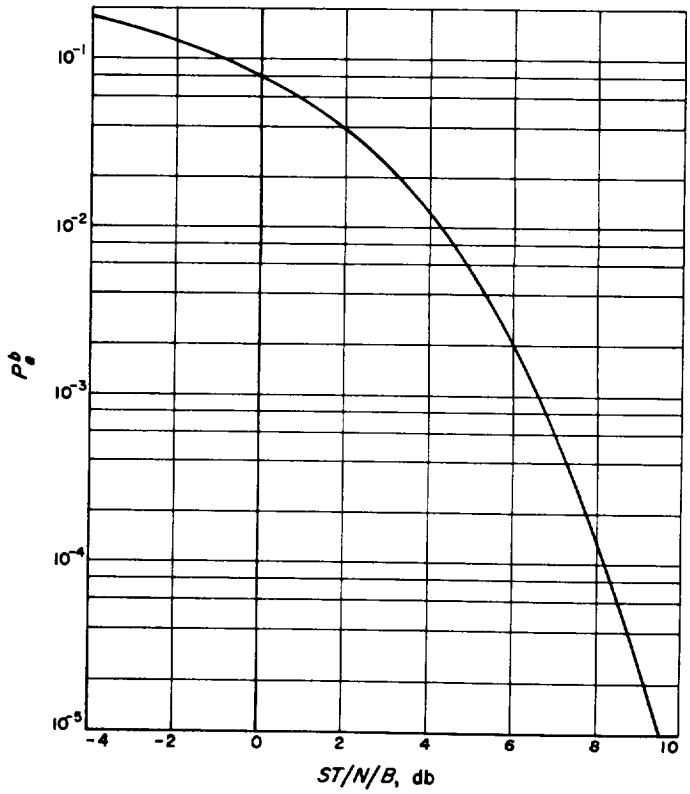

Fig. 3. Coherent PSK performance curve

A similar calculation for the command link, assuming that $P_e^b = 1 \times 10^{-5}$ and that the receiving antenna of the spacecraft is omnidirectional ($G_R = 0$ db), gives a data rate of 3.0 bps.

The telemetry and command data rates just obtained are only approximate since no attempt was made to optimize the RF carrier to sideband power ratio (equal powers were assumed), but they do show that even with an optimum choice of modulation and detection, the data rates are still very low when compared with those obtainable from satellites (tens of thousands of bits per second).

C. *The Detection and Synchronization Problem*

The elementary implementation of a coherent PSK system is shown in Fig. 4. The biorthogonal signals consist of a splitphase sinusoid such that $+\sin(\omega_0 t)$ is transmitted for the binary *one* and $-\sin(\omega_0 t)$ is transmitted for the binary *zero*. At the receiver, the noisy signal is correlated (multiplied) with the detector $+\sin(\omega_0 t)$ reference to obtain $1-\cos(2\omega_0 t)$ or $-1+\cos(2\omega_0 t)$. Only the dc terms of these expressions are of interest, since the matched filter following the coherent detector consists of an integrator, sample, and discharge configuration wherein the signal-to-noise ratio is maximized. [A matched filter for a signal embedded in Gaussian noise with uniformly flat power spectral density is a network such that its impulse response is the time-negative of the signal to be detected, in this case a rectangular pulse of duration T (Ref. 4). Since an integrator has a constant output for a single-impulse input, the complete matched filter consists of an integrator with discharge occurring at time T.] Bit synchronization or timing is required in the matched filter to sample and discharge the integrator properly.

The basic concept of phase-shift-keying is rather simple; the practical difficulty lies in obtaining the necessary bit sync and coherent demodulation reference within the detector with sufficient accuracy and stability. Should the detection reference, $\sin(\omega_0 t)$, be off in phase by an angle ϕ, then the efficiency of the detection process will be degraded by a factor of $\cos^2\phi$. If the bit synchronization timing for the matched filter is inaccurate, then

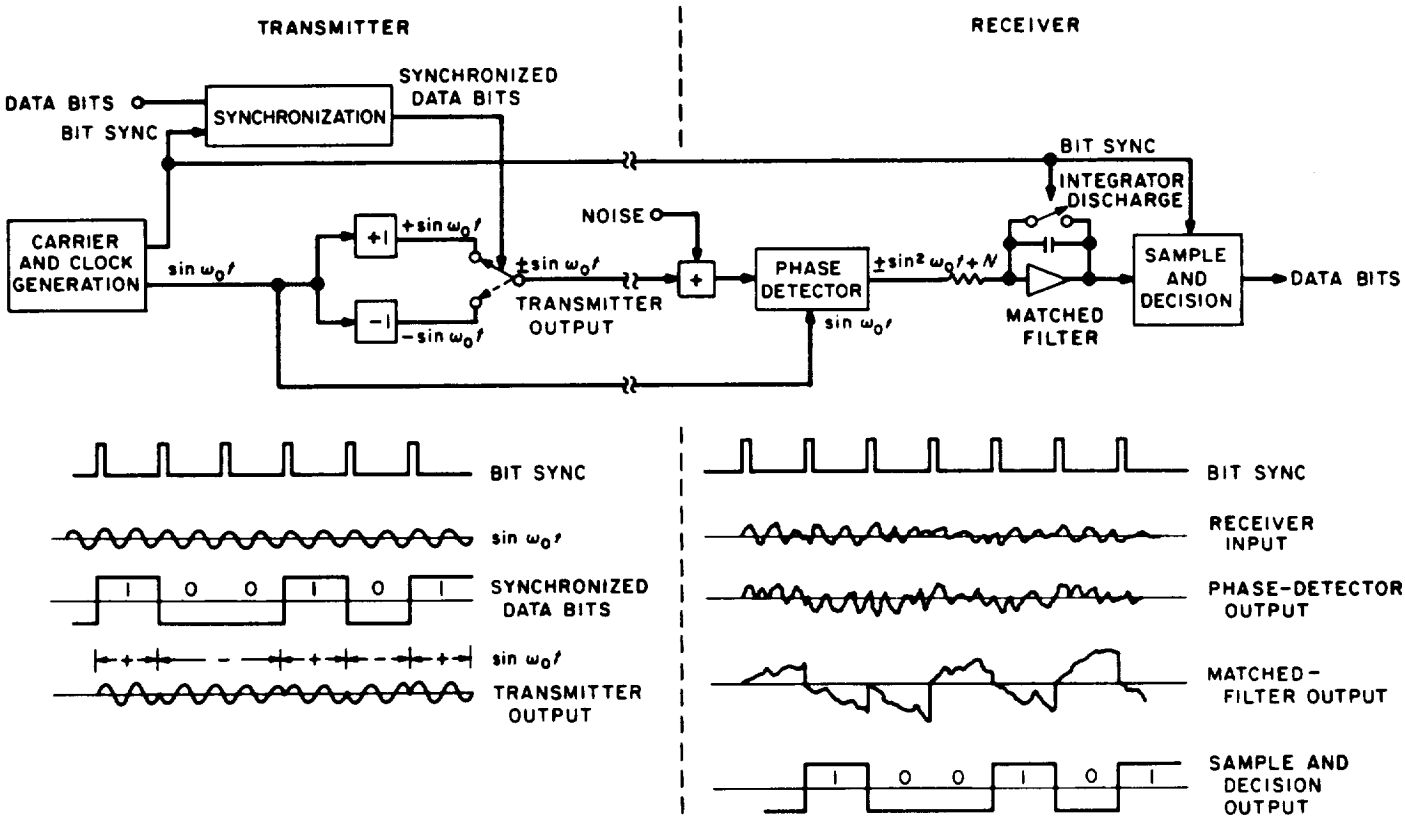

Fig. 4. Basic coherent PSK system

sampling may take place too soon or too late, thereby reducing the probability of making the correct decision. Also to be considered is any noise that may be on these signals, i.e., if the references possess jitter, then even further losses result. Consequently, if near-optimum performance is to be obtained, synchronization within the detector must be unique and as noise-free as possible.

Another important factor to consider when implementing the coherent PSK system is that the requirements for synchronization do not significantly degrade the theoretical system performance; in other words, if a certain amount of energy is available for the transmission of a data bit, plus establishing synchronization, then the latter should in effect require a minimum of the energy. Obviously, requirements for good synchronization and for minimum use of transmitter energy to obtain synchronization are somewhat in conflict.

In addition to the coherent reference and bit sync, word synchronization is required to separate the detected data bits into the proper groups. In fact, if word synchronization is available, bit sync may readily be obtained through the proper frequency multiplication process, and frame synchronization patterns (assuming frame synchronization patterns are placed within the data format) may be easily recognized.

During the past decade, a large number of binary codes have been devised and employed to achieve bit and word synchronization in PCM telemetry systems. In nearly all cases, the codes possess special autocorrelation properties through which synchronization may be uniquely and readily obtained. Examples of codes that have been employed are the comma-free codes and such transorthogonal codes as the pseudonoise (PN) and Legendre sequences. Usually, the code words are inserted at predetermined locations within the data format, and it is the function of the detection and decoding equipment to "search out," by means of correlation techniques, the correct code patterns.

Virtually all coded systems suffer from one or more drawbacks. When certain types of coding are used to derive word and frame synchronization, the decoding equipment may approach, in complexity, that of a digital computer, in order that synchronization can be achieved within a reasonable amount of time. Data transmission rates below several hundred bps are often hard to achieve because of the difficulty in detecting transitions at low signal-to-noise ratios (SNR's) to obtain bit synchronization. In addition, many systems are hybrid, using one type of code to obtain bit synchronization and another type to obtain word synchronization.

In order to circumvent these problems and meet the accuracy and stability criteria, a coherent PSK system has been developed wherein a maximal-length linear shift-register code is used in conjunction with phase-lock techniques to obtain both bit and word synchronization as well as a coherent demodulation reference. Emphasis has been placed on obtaining a detection system which does not require computer operations to obtain synchronization and which is capable of operating at very low data bit rates (1 bps) in a near-optimum manner.

IV. SYNCHRONIZATION THEORY

A. Code Properties

There exists a family of binary codes of length $4n - 1$ (where n is an integer) that are characterized by their two-level autocorrelation properties (Ref. 5). Perhaps the most widely known subclasses of this family are the codes of length $2^n - 1$, many of which, in addition to having two-level autocorrelation, possess the cycle-and-add property (Ref. 6). These codes are often referred to as maximal-length linear shift-register codes or PN codes.

The cycle-and-add property has the characteristic that given a PN code of length $2^n - 1$ and any cyclic permutation of the same PN code, the modulo-2 (mod-2) sum is another cyclic permutation of the PN code. For example, consider a length 7 PN code, 1110100, and a cyclic permutation, 1010011; forming a mod-2 sum, we have

$$\begin{array}{r} 1110100 \\ 1010011 \\ \hline 0100111 \end{array}$$

where the result, 0100111, is a cyclic permutation of 1110100.

For a code possessing the cycle-and-add property, once n of the sequential states have been established, all succeeding states may be uniquely predicted through the proper mod-2 process, i.e., given the sequence

$$a_n \cdots a_k \cdots a_3 a_2 a_1 \tag{7}$$

there exists a single k such that

$$a_{n+1} = a_k \oplus a_1 \tag{8}$$

where the symbol $\oplus$ denotes mod-2. This property provides an easy method of generating PN codes by employing an n-stage shift register and mod-2 feedback as shown in Fig. 5. Note that the $000 \cdots 0$ word cannot be permitted to occur.

Values of a_k for generating codes up to length 2047 appear in Table 2. The $2^n - 1$ length codes which possess two-level autocorrelation, but which do not have cycle-and-add properties, require more than two shift-register stage outputs for generation; these may be obtained from tables of irreducible primitive polynomials over $GF(2)$ (Ref. 7). For simplicity, we will deal subsequently only with the PN codes possessing the cycle-and-add property, although the final results obtained are also applicable to all other PN codes.

The PN code generator clock or drive frequency will now be defined and will be referred to as $2f_s$. Two other frequencies, f_s and $f_s \angle 90$ deg, are defined such that

$$2f_s = f_s \oplus f_s \angle 90 \text{ deg} \tag{9}$$

Table 2. PN code shift-register generator feedback connections

$2^n - 1$	a_1	a_k
3	2	1
7	3	1, 2
15	4	1, 3
31	5	2, 3
63	6	1, 5
127	7	1, 3, 4, 6
511	9	4
1023	10	3, 7
2047	11	2, 9

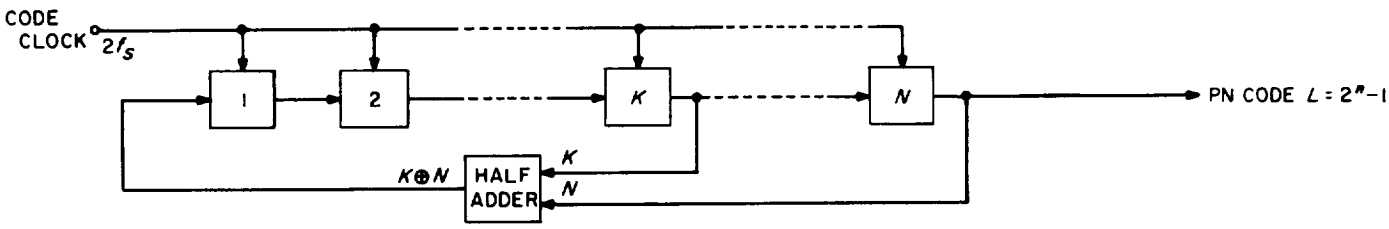

Fig. 5. Shift-register generator

These relationships are shown in Fig. 6, together with a length 15 PN code.

The normalized time autocorrelation $R(\tau)$ of a function $f(t)$ is defined generally by

$$R(\tau) = \frac{1}{K} \lim_{T \to \infty} \frac{1}{T} \int_0^T f(t) f(t + \tau) dt \qquad (10)$$

where

$$K = \lim_{T \to \infty} \frac{1}{T} \int_0^T f^2(t) dt \qquad (11)$$

When $f(t)$ is a periodic binary code (composed of *ones* and *zeros*) of length L, the normalized autocorrelation may be written as

$$R(\tau) = 1/L \text{ Ave } \{\text{code} \oplus \text{code}(\tau)\} \qquad (12)$$

where Ave { } is defined to mean the number of *zeros* minus the number of *ones* in code $\oplus$ code(τ). It is not necessary to confine τ strictly to integer values of the bit period, since the code can always be expanded by replacing each *one* by *n ones* and each *zero* by *n zeros* to obtain $R(\tau)$ for fractional values of τ.

The fact that a PN code has a two-level autocorrelation function may now be shown. Since Ave {PN$\oplus$PN} = L, then $R(0) = 1$ for $\tau = 0$. The number of *ones* in a PN code is $2^n/2$, and the number of *zeros* is $(2^n - 2)/2$. Now, for integer values of τ, PN$\oplus$PN(τ) = PN(τ') since the codes possess the cycle-and-add property; therefore

$$R(\tau') = [(2^n - 2)/2 - 2^n/2]/L = -1/L \qquad (13)$$

Inspection of PN codes shows that the autocorrelation is uniformly linear between the integer τ values. This autocorrelation function is plotted in Fig. 7.

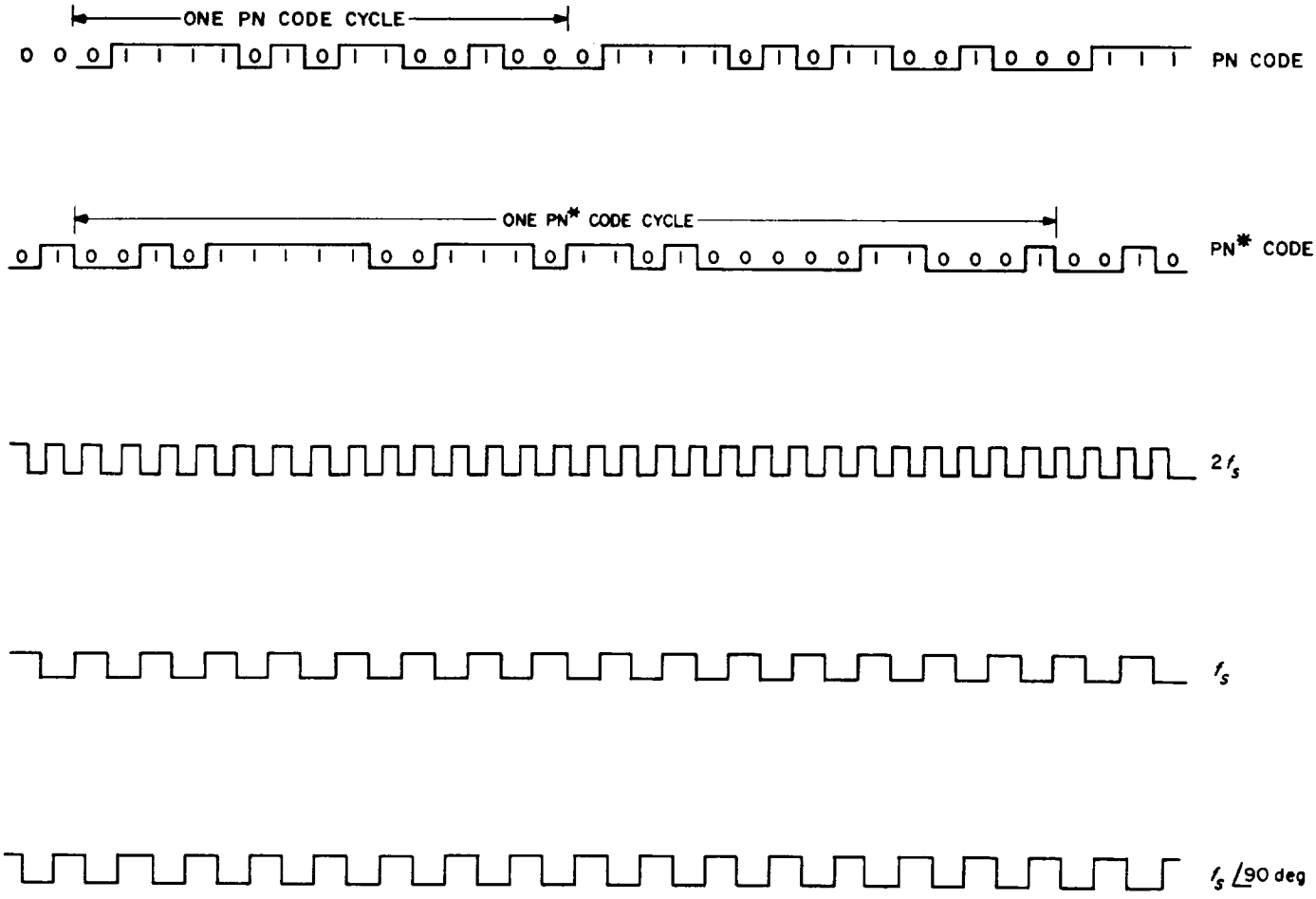

Fig. 6. Code and clock relationships

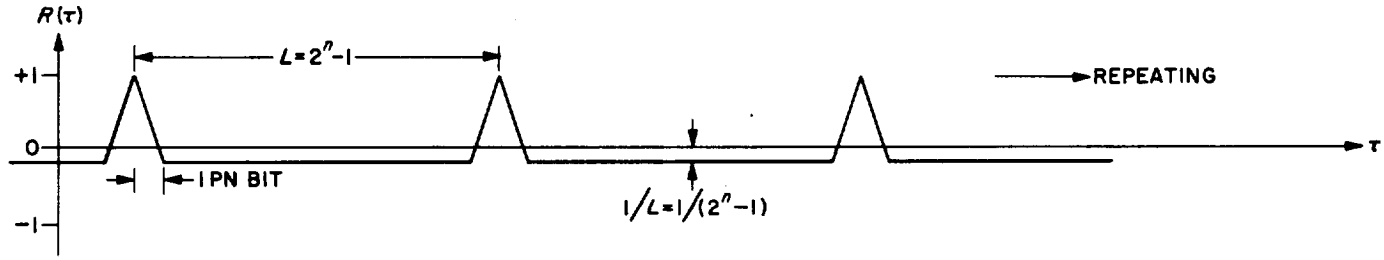

Fig. 7. PN autocorrelation function

The code PN* will now be defined as PN$\oplus f_s$. Since PN is of odd length and there is a half cycle of f_s for each PN bit, PN* will have a cycle length of $2L$, being composed of a code of length L, followed by its complement. An example of the PN* code is shown in Fig. 6.

The autocorrelation function for the PN* code may be derived from the autocorrelation function of the PN code in the following manner. Now,

$$R^*(\tau) = \text{Ave } \{\text{PN}^* \oplus \text{PN}^*(\tau)\}/L \tag{14}$$

and

$$\text{PN}^* \oplus \text{PN}^*(\tau) = \text{PN} \oplus \text{PN}(\tau) \oplus f_s \oplus f_s(\tau) \tag{15}$$

For $\tau = 2K$; $K = 0, 1, 2, 3, \cdots$

$$f_s \oplus f_s(2K) = 00000\cdots \tag{16}$$

and for $\tau = 2K - 1$; $K = 0, 1, 2, 3, \cdots$

$$f_s \oplus f_s(2K) = 11111\cdots \tag{17}$$

Therefore,

$$R^*(2K) = \text{Ave } \{\text{PN} \oplus \text{PN}(2K)\}/L \tag{18}$$

and

$$R^*(2K - 1) = -\text{Ave } \{\text{PN} \oplus \text{PN}(2K - 1)\}/L \tag{19}$$

As a result, the PN* autocorrelation function is obtained from the PN autocorrelation function by plotting the PN autocorrelation for all $\tau = 2K$, and the negative of the PN autocorrelation for all $\tau = 2K - 1$, with the intermediate values being uniformly linear. The PN* autocorrelation function is shown in Fig. 8. Note that the points of maximum correlation cycle between +1 and −1 and occur for each cycle of the PN code component.

The autocorrelation properties of PN* codes provide the basis by which two identical PN code generators operating from independent clock sources can be locked in time synchronism. Consider the following code and clock combinations:

$$\text{PN} \oplus 2f_s = \text{PN} \oplus f_s \oplus f_s \angle 90 \text{ deg} = \text{PN}^* \oplus f_s \angle 90 \text{ deg} \tag{20}$$

The cross-correlation function of two different codes may be written in a form similar to that of the autocorrelation function as

$$C(\tau) = 1/L_{12}\text{Ave } \{\text{code}_1 \oplus \text{code}_2(\tau)\} \tag{21}$$

where L_{12} is the product of the lengths of the two codes.

The cross-correlation between PN$\oplus 2f_s$ and PN will now be derived. With τ = integer values, PN$\oplus 2f_s \oplus$PN(τ) = PN$(\tau')\oplus 2f_s$, because of the cycle-and-add property. Since there is exactly one cycle of

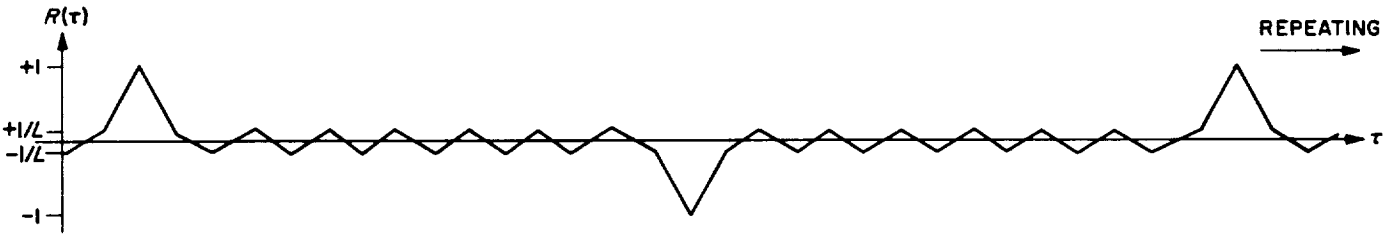

Fig. 8. PN* autocorrelation function

$2f_s$ for each PN bit, and the Ave $\{2f_s\}$ per PN bit is zero, then $C(\tau) = 0$ for all τ = integers. Since $C(\tau)$ is zero for integer values, and since Ave $\{PN \oplus PN(\tau)\}$ is uniform for both integer and fractional values of τ over the region $1 \leq |\tau| \leq L - 1$ (L = length of PN code), then $C(\tau)$ must also be zero for the noninteger values of τ.

The only region left to be examined is $0 < |\tau| < 1$. The two waveforms, which are one cycle of $2f_s$ and one PN bit that is chosen as a *one*, are of interest over this interval. Outside the interval, all states are now equally likely, since the remaining portion of the PN code contains an equal number of *ones* and *zeros*. The value $C(\tau)$ need only be evaluated over the interval for which $PN \oplus 2f_s \oplus PN(\tau)$ is nonbalanced (see Fig. 9), which requires calculating only the cross-correlation between one $2f_s$ cycle and one PN bit.

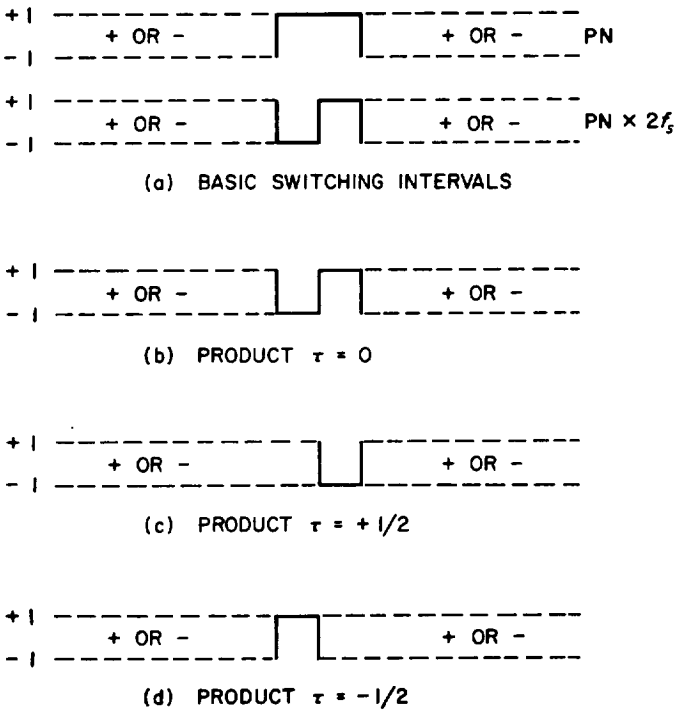

Fig. 9. Examples of cross-correlation calculation

The complete cross-correlation function is shown in Fig. 10. It can be seen that an S-curve is generated each time the PN code passes through its point of maximum correlation; otherwise, the function is zero. This property is ideal for employing phase-lock techniques to synchronize the two PN code generators, with the cross-correlation function forming the loop error signal.

B. *Elements of Second-Order Phase-Locked Loops*

Many excellent references (Ref. 8–12), are available on the theory and operation of phase-locked loops. As a result, only a few fundamentals of second-order loops will be presented here, and the reader is directed to the above-listed references for further detail.

The basic phase-locked loop (PLL), together with its pertinent signal equations, appears in Fig. 11. The input and output signals are usually represented by sinusoids for the purpose of analysis, but this is not restrictive in practice, and in fact, it is often more convenient to use square waves.

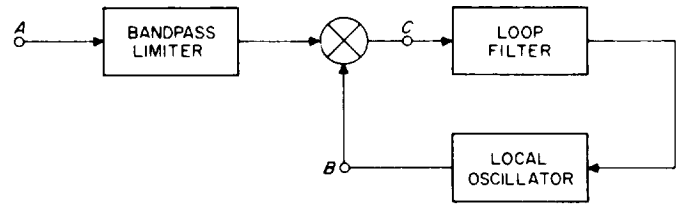

$$A(t) = \sqrt{2}A \sin\left[2\pi f_i t + \theta_i(t)\right] \quad (1)$$

$$B(t) = \sqrt{2}B \cos\left[2\pi f_0 t + \theta_0(t)\right] \quad (2)$$

$$C(t) = K_m \sin\left[\theta_i(t) - \theta_0(t)\right] \quad (3)$$

$$K_m = K \cdot A \cdot B \quad (4)$$

Fig. 11. Basic phase-locked loop

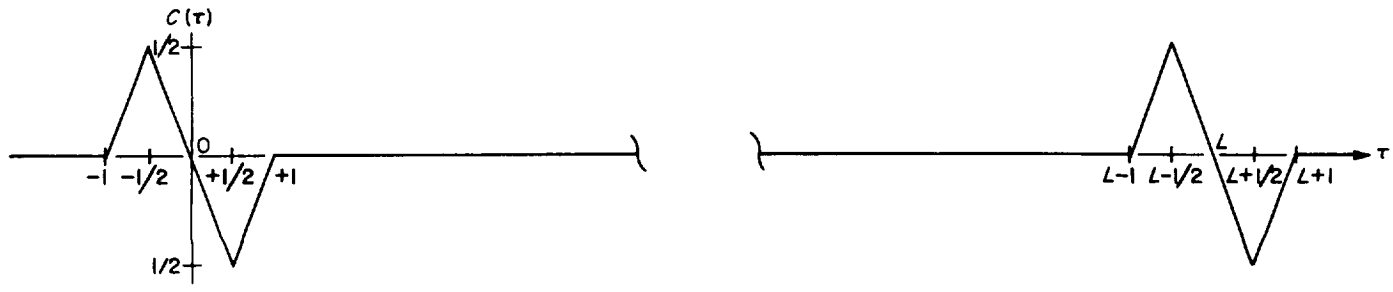

Fig. 10. Cross-correlation function

In the absence of noise at the input, the operation of the loop is relatively easy to explain. The loop error signal formed by the product of the input and reference signals is proportional to their phase differences. The loop filter following the multiplier acts effectively as a low-pass filter, which eliminates the second harmonic of the error signal, prior to application of the error signals to the input of the voltage-controlled oscillator (VCO). The error signal serves to drive the frequency and phase differences between the input and reference signals to zero, i.e., $\omega_0 \doteq \omega_i$ and $\theta_0 = \theta_i$. Once this has been accomplished, the error signal becomes zero, and the loop is said to be locked.

If the loop is opened, and $\omega_0 \neq \omega_i$, then the error signal (neglecting the second harmonic) is a sine wave in time and is representative of the cross-correlation between the input and reference signals. When the input and reference signals are square waves, the loop error signal is in the form of a triangular wave (see Fig. 12).

The loop error signal is zero at multiples of π, but since the slopes at these points are alternately positive and negative, the lock points can occur for the correct slope only at multiples of 2π.

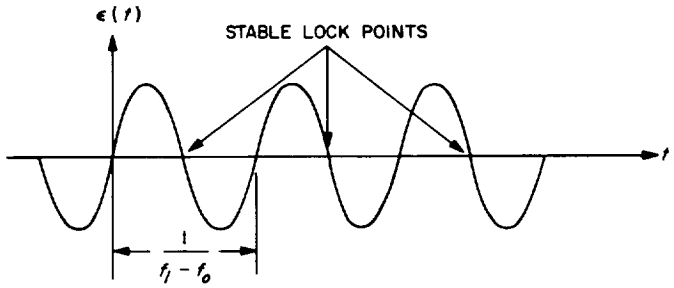

(a) SINE WAVE INPUTS

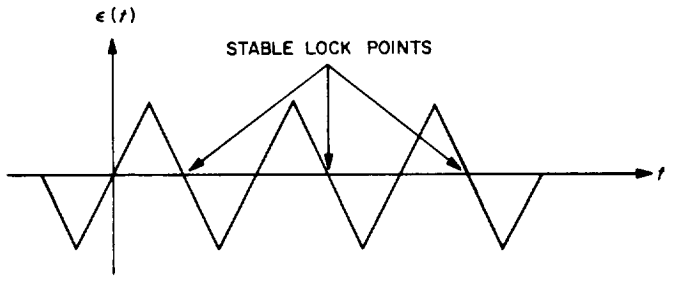

(b) SQUARE WAVE INPUTS

Fig. 12. Loop error signal

For the sake of analysis, the loop is generally linearized as shown in Fig. 13, which assumes the approximation that $\sin\theta \approx \theta$ is valid. The multiplier is replaced by a summing network, the VCO by an integrator, the loop filter by a network designated $F(s)$, and all dc gain or loss by a single amplifier. When the loop is optimized by minimizing the rms phase jitter, σ_n, plus the transient error (due to input frequency steps) on the reference signal, using Wiener mean-square error techniques, $F(s)$ becomes

$$F(s) = \frac{B_0^2 + \sqrt{2}B_0 s}{Gs} \tag{22}$$

where B_0 is the natural frequency of the loop in radians per second. The closed-loop transfer function is then given by

$$H(s) = \frac{\theta_0(s)}{\theta_i(s)} = \frac{B_0^2 + \sqrt{2}B_0 s}{B_0^2 + \sqrt{2}B_0 s + s^2} \tag{23}$$

The loop noise equivalent bandwidth is important in determining the threshold of the loop with a signal-plus-noise input, and is obtained from $H(s)$ as

$$2B_L = \frac{1}{|H(0)|^2}\int_{-\infty}^{\infty} |H(s)|^2 ds = 1.06\, B_0 \tag{24}$$

The approximate relationship between the SNR in the loop and σ_n when $(S/N)_{2B_L} > 10$ db is

$$(S/N)_{2B_L} = 1/2B_L\Phi_N \approx 1/2\sigma_n^2 \tag{25}$$

where Φ_N is the normalized phase noise-to-signal ratio $(N/B)/S$ at the frequency input to the loop.

The threshold of the loop is difficult to define. Practically, a threshold is obtained when the loop no longer functions as intended. The "absolute threshold" is generally considered to occur when the signal-to-noise ratio

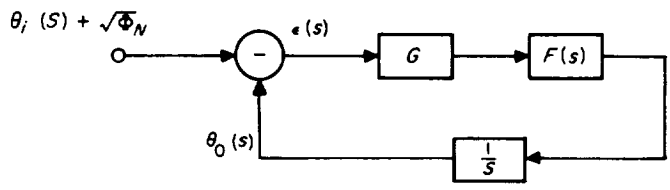

Fig. 13. Linearized phase-locked loop

in $2B_L$ reaches 0 db. At this point $\sigma_n \simeq 1$ rad rms, and the loop is out-of-lock a certain percentage of the time. This condition is often referred to as "skipping cycles," i.e., the noise drives the loop past the 90-deg point of the loop error signal (Fig. 12) so that lock cannot be regained until the next (or perhaps the second or third) lock point is reached.

The noise bandwidth of the loop, $2B_L$, is a function of the loop gain, which in turn is dependent upon input signal voltage. Since the input signal voltage may vary over a period of time, it is desirable to provide a means of making $2B_L$ somewhat insensitive to such variations. As a result, a bandpass limiter is usually placed ahead of the multiplier or phase detector to hold the total signal-plus-noise voltage into the loop constant. With a bandpass limiter, the loop noise bandwidth now becomes dependent upon signal-to-noise ratio in accordance with the limiter suppression effect (Ref. 13). A curve relating the output SNR to the input SNR through a bandpass limiter appears in Fig. 14, and the curve in Fig. 15 shows the signal voltage suppression factor, α, to the SNR in the limiter bandwidth.

The threshold loop noise bandwidth will now be designated as $2B_{Lo}$, corresponding to a suppression factor α_0. Above threshold, the equation relating $2B_L$ to $2B_{Lo}$ is

$$2B_L/2B_{Lo} = \frac{1}{3}\left(1 + 2\frac{\alpha}{\alpha_0}\right) \qquad (26)$$

Finally, the loop filter $F(s)$ may be realized by the passive circuit configuration shown in Fig. 16. The filter time constants are related to $2B_{Lo}$ by

$$T_1 = R_1C = 1.12\, G_0/(2B_{Lo})^2 \qquad (27)$$

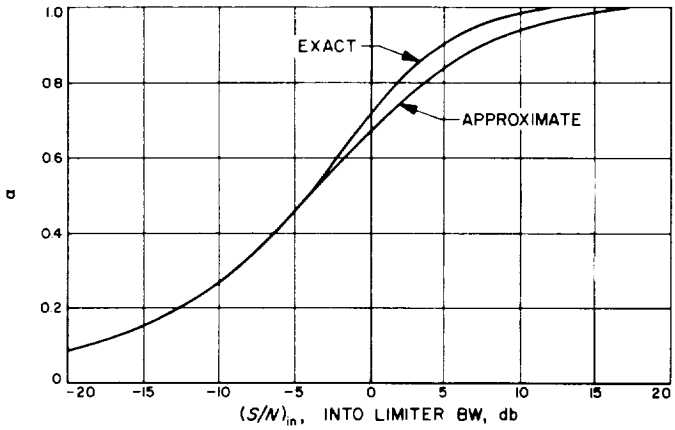

Fig. 15. Signal suppression factor for an ideal limiter

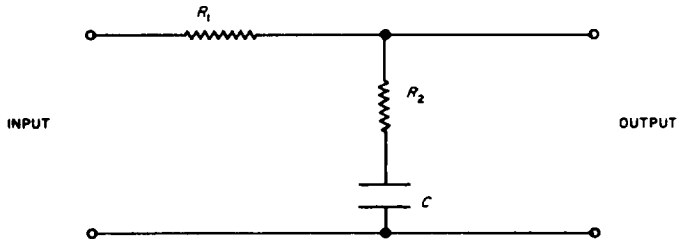

Fig. 16. Passive loop filter

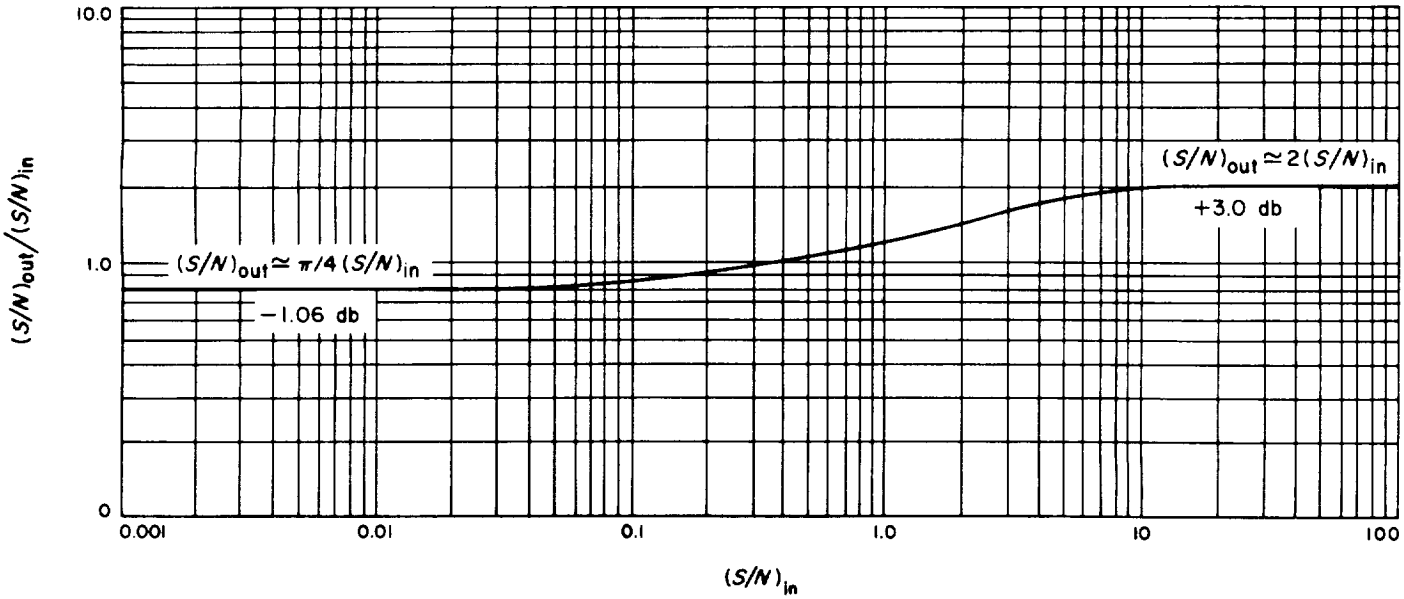

Fig. 14. S/N relationships in an ideal bandpass limiter

and

$$T_2 = R_2C = 1.5/2\,B_{L0} \qquad (T_1 >> T_2 >> 1) \qquad (28)$$

where

$$G_0 = G\alpha_0 = K_M K_{VCO} K_a \alpha_0 \qquad (29)$$

K_M = multiplier constant, v/rad

K_{VCO} = VCO constant, rad/sec/v

K_a = any miscellaneous dc gain or loss

Now that code properties and the operation of phase-locked loops have been described, the complete sync system will be discussed.

C. The Basic Sync System

The modulator and detector of the basic synchronization system appear in Fig. 17.

The modulator consists of a $2f_s$ clock, a PN code shift-register generator, and a mod-2 adder, the output of which is PN$\oplus 2f_s$.

The detector is a two-loop, phase-lock system. The input signal, PN$\oplus 2f_s$, is first correlated, or multiplied by, PN* to obtain $f_s \angle 90$ deg when the modulator and detector PN codes are aligned. Note that some form of analog multiplier must now be used in place of the mod-2 adder, since the input signal will generally be noisy. The $f_s \angle 90$ deg signal is passed through a filter–limiter combination, following which it is multiplied by f_s to form the error signal. Although the error signal could be derived by directly multiplying PN$\oplus 2f_s$ by PN, it is broken here into two parts in order to incorporate the filter–limiter.

Now, if the second loop is opened, and the VCO frequency is slightly different from that of the modulator $2f_s$ clock, the cross-correlation function of Fig. 10 will appear in time at the output of the second multiplier. By comparison with the loop error signal of the normal second-order PLL, it can be seen that the PN-locked loop possesses a lock point only when the received and local PN codes are in time synchronism. To acquire the PN system, then, one closes the loop and sets a frequency difference, Δf, between the VCO and the modulator $2f_s$ clock so that the received and local codes can drift in time relative to one another until lock is obtained.

Since locking of the PN code synchronization system is unique, word detectors placed on each of the PN shift-register generators serve to provide unambiguous bit- and word-sync pulses when the PN generators cycle at the word rate. Also, since the $2f_s$ clocks, and any harmonic thereof, are phase-coherent, a data demodulation reference may be obtained. This will be elaborated on in Sections V and VI.

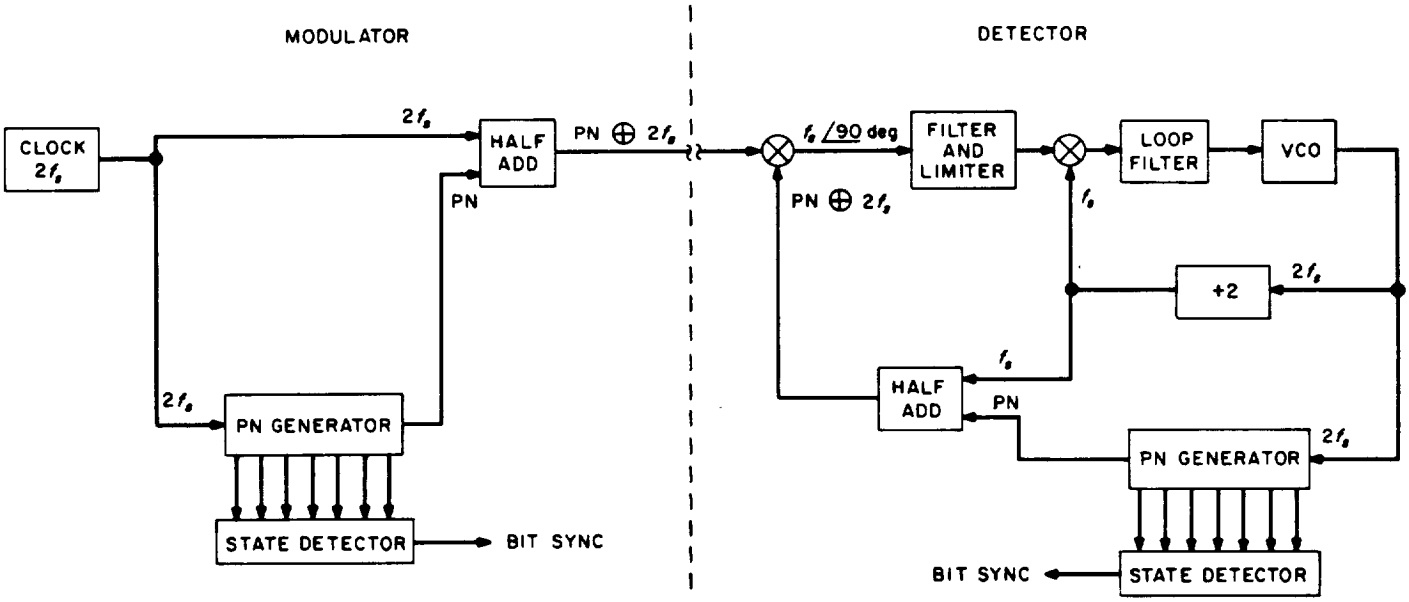

Fig. 17. Basic sync system

D. Acquisition Properties

A brief note should be made here concerning the acquisition properties of the basic sync system. The maximum frequency difference, Δf, between the VCO and the modulator $2f_s$ clock is related to the noise bandwidth of the loop, and a restriction placed upon acquisition is that lock be obtained on the first code correlation. To obtain Δf, one must solve by analog or digital computer techniques the nonlinear equation describing the loop (Ref. 11, 14). The results are in the form of phase-plane diagrams and describe the acquisition under no-noise conditions only. For the loop error signal of the PN system, it has been shown (Ref. 15) that

$$\Delta f < 2B_{Lo}/1.06 \tag{30}$$

to acquire lock at the first lock-point encountered. Under noisy conditions approaching the threshold of the loop (which will be defined later) it has been found empirically that Δf should be constrained to be less than about $2B_{Lo}/2$.

E. Power Spectral Density

The power spectral density envelope of PN$\oplus 2f_s$ must be determined in order to specify a transmission bandwidth. Two methods are available for calculating the power spectral density, (1) the Fourier transform of the autocorrelation function and (2) the Fourier transform squared of the basic switching waveforms. The latter method is most convenient here since the autocorrelation function is more difficult to handle because it must be broken into line segments of different slopes. The Fourier transform of the autocorrelation function, however, readily gives the power spectrum envelope of the PN code itself, since the Fourier transform of a triangular autocorrelation function is well known and gives

$$G(f)_{PN} = \frac{\sin^2(\pi f/2f_s)}{(\pi f/2f_s)^2} \tag{31}$$

(It should be pointed out that the spectrums under consideration are, in reality, line spectrums, but that the line density is so high that their envelopes adequately describe them.)

The method employed to obtain the power spectrum of PN$\oplus 2f_s$, outlined elsewhere (Ref. 16), considers the Fourier transform of a basic switching interval, in this case one cycle of $2f_s$, and weights the transform with the probability of being in the state under consideration. The sum of all weighted transforms, in this case two, then becomes the complete spectrum. Thus,

$$G(f)_{PN\oplus 2f_s} = 4f_s \sum_{i=1}^{2} p_i |H_i(f)|^2 \tag{32}$$

where

$$H_i(f) = \int_0^{1/2f_s} h_i(t) \exp(-j2\pi ft)dt \tag{33}$$

and $h_i(t)$ is the waveform in the basic switching interval. Since $|H_i(f)|^2$ is the same for both phases of $2f_s$, and $p_1 + p_2 = 1$, we have

$$G(f)_{PN\oplus 2f_s} = 4f_s \left| \int_0^{1/4f_s} \exp(-j2\pi ft)dt - \int_{1/4f_s}^{1/2f_s} \exp(-j2\pi ft)dt \right|^2 \tag{34}$$

$$= \frac{1}{f_s} \frac{\sin^4(\pi f/4f_s)}{(\pi f/4f_s)^2} \text{ w/cps}$$

A normalizing factor has been included to make

$$\int_0^{\infty} G(f)_{PN\oplus 2f_s} \equiv 1 \tag{35}$$

Both $G(f)_{PN\oplus 2f_s}$ in watts/cps and the cumulative power are plotted in Fig. 18. As can be seen, the cumulative power between 0 and the first spectral null, $4f_s$, is approximately 85.6% of the total power, and therefore 0 to $4f_s$ cps will be defined as the minimum required transmission bandwidth.

Another form of PN$\oplus 2f_s$ that will be useful when mechanizing single-channel systems (Section VI) is PN* $\times$ $f_s\angle 90$ deg, where PN* is as previously defined and $f_s\angle 90$ deg is now a sine wave. (The multiplication sign $\times$ is used to indicate that one of the waveforms is nonbinary.) The spectrum, using the same method as above, is derived as

$$G(f)_{PN^*\times f_s\angle 90\,\text{deg}} = \frac{4}{\pi} \frac{(f/f_s)^2 \cos^2(\pi f/2f_s)}{[1-(f/f_s)^2]^2} \tag{36}$$

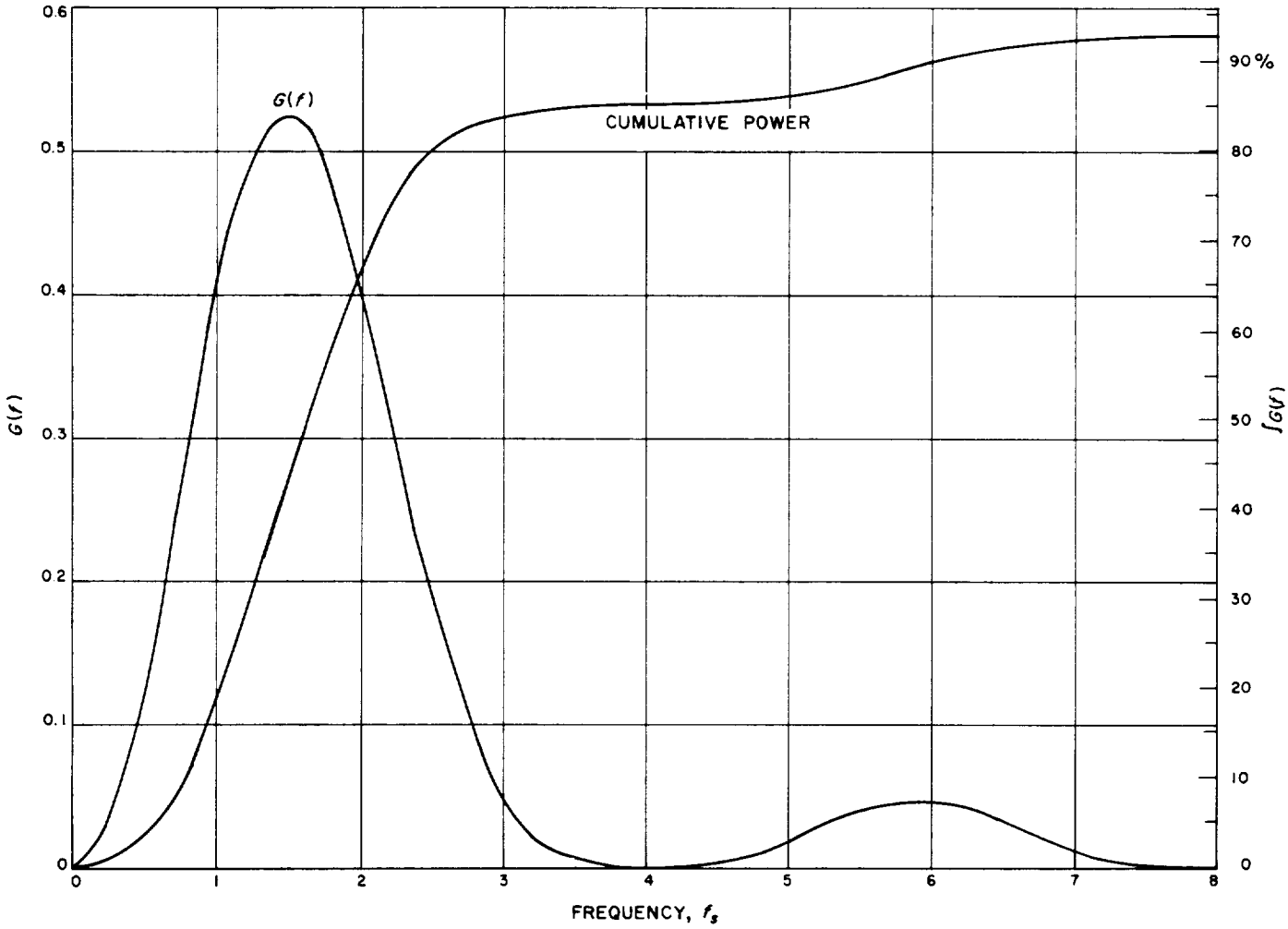

Fig. 18. Power spectral density and cumulative power for PN⊕2f_s

Fig. 19 shows a plot of $G(f)_{PN^* \times f_s \angle 90\,deg}$ in watts/cps and the cumulative power. Note that the first spectral null now occurs at $3f_s$ rather than at $4f_s$ as was the case for PN⊕2f_s. The cumulative power between 0 and $3f_s$ is approximately 85.9% of the total power, so that 0 to $3f_s$ will be defined as the minimum required transmission bandwidth.

F. Noise Performance

Predicting the noise performance of the sync system is just as difficult as, if not more so than, predicting the performance of a simple phase-locked loop. Therefore, many of the results have been arrived at experimentally.

First, the SNR in the PLL noise bandwidth must never be allowed to reach a value where there is a good probability of skipping cycles, which in this case means complete loss of lock because of the discontinuous loop error signal. If we choose to say that the probability of remaining in lock is 6σ, then the 1σ or rms value of the phase jitter in the loop must be 15 deg. From Eq. (25) this results in

$$(S/N)_{2B_{L_0}} \approx 9.0 \text{ db}$$

which is very far above the absolute threshold of 0 db for the normal PLL.

To specify the input SNR to the whole detector, it is necessary to include the SNR change through the filter–limiter combination, plus the fact that PN* also possesses phase jitter. The phase jitter on PN* complicates the analysis of the system, since it is correlated with the phase jitter in the loop, and as a result, an exact analytical solution for the entire detection system is very difficult,

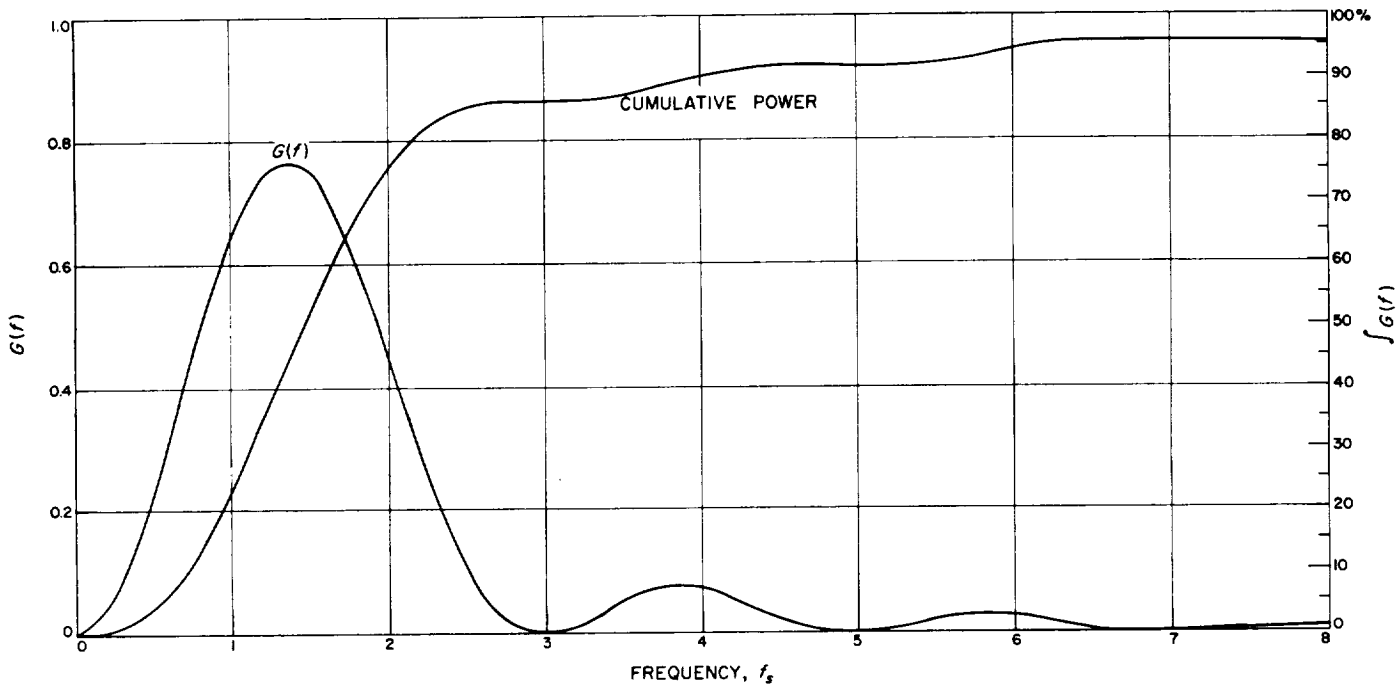

Fig. 19. Power spectral density and cumulative power for PN* × f_s∠90 deg

if not impossible, to obtain. However, empirical results have indicated that

$$(S/N)_{2B_{L_0}}\,(\text{min}) \approx 9.0\ \text{db}$$

(taking into account the suppression factor) at the input to the detector in order to obtain the desired performance. If

$$(S/N)_{2B_{L_0}} < 9.0\ \text{db}$$

acquisition of the code at the first lock-point has been experimentally determined to be difficult. As a result,

$$(S/N)_{2B_{L_0}} = 9.0\ \text{db} \tag{37}$$

at the input to the double-loop detector will be defined as the absolute threshold of the sync system.

V. TWO-CHANNEL SYSTEMS

A. Two-Channel Mechanization

The two-channel system represents the first operational use of the basic sync system for both telemetry and command functions on the *Mariner 2* spacecraft (Ref. 17) that achieved a successful rendezvous with the planet Venus on December 14, 1962. Although the two-channel system does not represent the optimum method of embodying the telemetry or command data, it will be outlined here because of its historical significance. Before proceeding, however, to the actual data-modulation and detection techniques, a more detailed discussion of the relationship between the PN code length and the data bit period is necessary. This may best be accomplished through the use of some examples.

First consider an application wherein only bit sync is required and a data bit rate of 50 bps is desired. A PN code may now be chosen, together with the appropriate $2f_s$ clock frequency, to cycle at the data rate of 50 bps, e.g., $L = 31$ and $2f_s = 1{,}550$ cps. Thus, a single word detector placed upon the PN code generator will provide 50 pulses per second (pps) representing bit sync.

Another way in which a rate of 50 pps can be obtained is by letting $L = 63$ and $2f_s = 1{,}050$ cps and placing three word detectors on the PN generator. (Note: $63 = 3 \times 21$.) The advantage of this choice over the former is that less transmission bandwidth is required to accomplish the same result, while the disadvantage is that the PN acquisition time is approximately doubled.

Now suppose a word-synchronous system is wanted, where a group of 7 data bits is a data word. In this case, the PN code length would be chosen so that it was divisible (or nearly divisible) by 7 and would cycle at the word rate, e.g., $L = 63$ and $2f_s = 450$ cps for a 50-bps system, with six word detectors on the PN generator providing the intermediate bit sync pulses and one word detector to provide the word sync pulse.

It should be pointed out here that the basic sync system is not conservative of bandwidth, i.e., the number of synchronizing PN bits required in conjunction with the actual information or data bits is significantly larger, and in some applications this might become a serious draw-

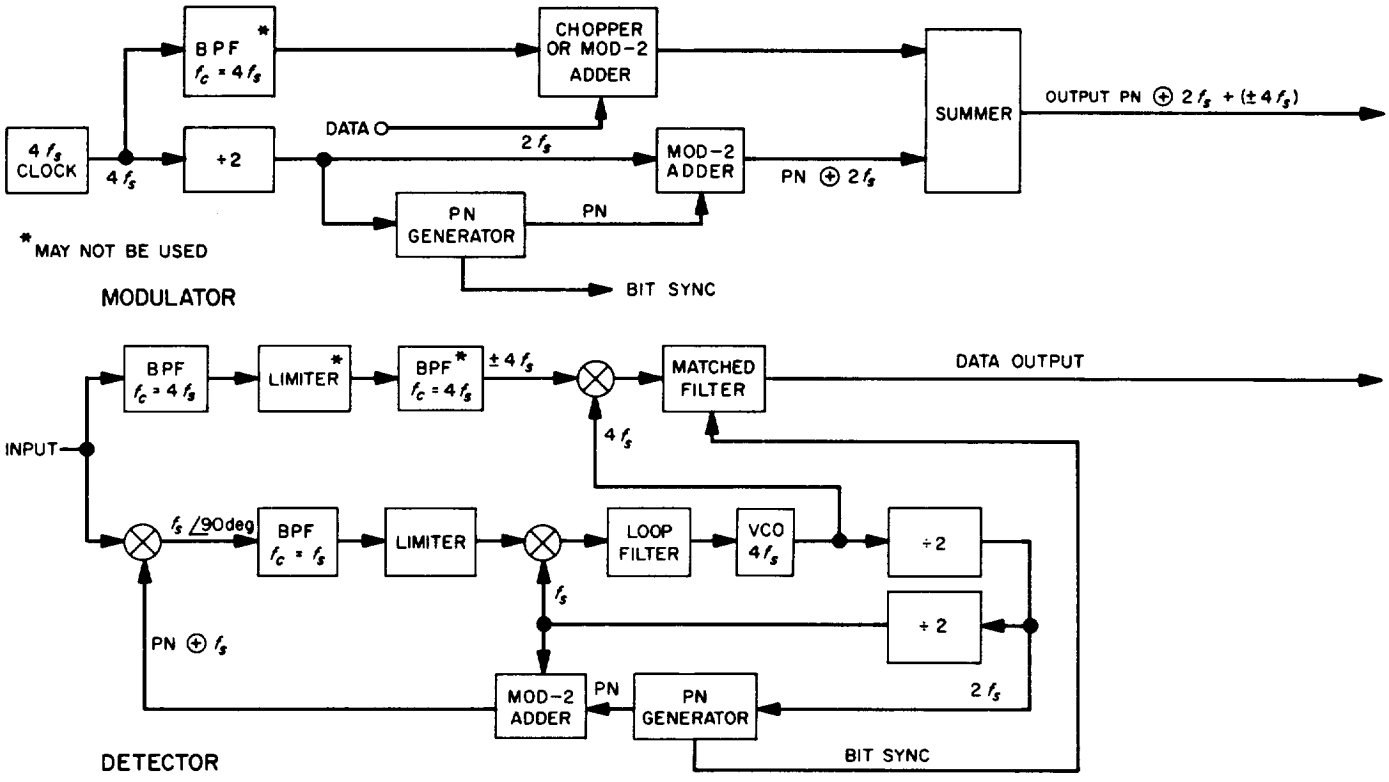

Fig. 20. Two-channel modulation and detection systems

back. For applications to planetary space vehicles, however, accuracy and efficiency are the most important factors, and bandwidth has been a secondary consideration to date.

A block diagram showing the system configuration for the two-channel modulator and detector appears in Fig. 20. Because of the broad spectral null in the PN$\oplus 2f_s$ sync spectrum at $4f_s$, a coherent $4f_s$ subcarrier is inserted to provide the data channel. The generation of the PN code and synchronization in the modulator is identical with that previously described. The data subcarrier is obtained by filtering the $4f_s$ square wave, and bi-phase modulation is accomplished by means of a chopper switch. The output of the modulator consists of the combined data and synchronization signals in the form

$$k_1 (\text{data} \times 4f_s) + k_2 (\text{PN} \oplus 2f_s)$$

where k_1 and k_2 are weighting constants that allocate the proper amount of available transmitter sideband power to each signal.

At the detector input, both signals enter the synchronization portion of the system, where multiplication by PN* occurs. No attempt to filter out the data subcarrier is made since the net effect of multiplying the $4f_s$ data subcarrier by PN* is to spread the data subcarrier over a wide frequency range so that no significant interference with the recovered $f_s \angle 90$ deg to the PLL is obtained. The remaining portions of the sync detection system operate as previously described.

A bandpass filter selects the modulated data subcarrier from the detector input spectrum, and after passing through a limiter and a second filter in order to limit the dynamic range, the subcarrier is coherently demodulated and passed to the matched filter and decision circuits.

B. Performance

It is natural to attempt to minimize k_2 so that the data channel will receive most of the available transmitter sideband power. However, a serious problem arises when k_2 is chosen so that the sync loop operates at its absolute threshold of 9 db in $2B_{Lo}$. Since the rms phase jitter on f_s is 15 deg, the rms phase jitter on the data channel $4f_s$ demodulation reference is 60 deg. This amount of phase jitter very significantly degrades the performance of the data channel. Assuming that the loss introduced by the phase jitter is independent of the data channel noise, and that the phase jitter has a Gaussian distribution, the loss may be calculated by means of weighted statistical averages. The problem, then, is to obtain the statistical average of the product of a sine wave, phase-modulated by Gaussian noise, and a sine wave of the same frequency and phase, but unmodulated. The solution has been obtained (Refs. 4, 18), and the results show that

$$(S/N)_{\text{loss}} = \exp(\theta^2) - 1 \qquad (38)$$

where θ is the rms phase jitter (in radians) on the demodulation reference. Figure 21 is a plot of the loss equation in decibels. As can be seen, the loss for $\theta = 60$ deg $= 1.05$ rad is 4.75 db, which obviously cannot be tolerated.

A more practicable value for the loss due to the reference phase jitter might be 0.5 db, which would require $\theta = 0.34$ rad and corresponds to a SNR in $2B_{Lo}$ of 18.4 db. To obtain this SNR requires that the sync power be raised by a factor of 8.71, or that $2B_{Lo}$ be lower by the

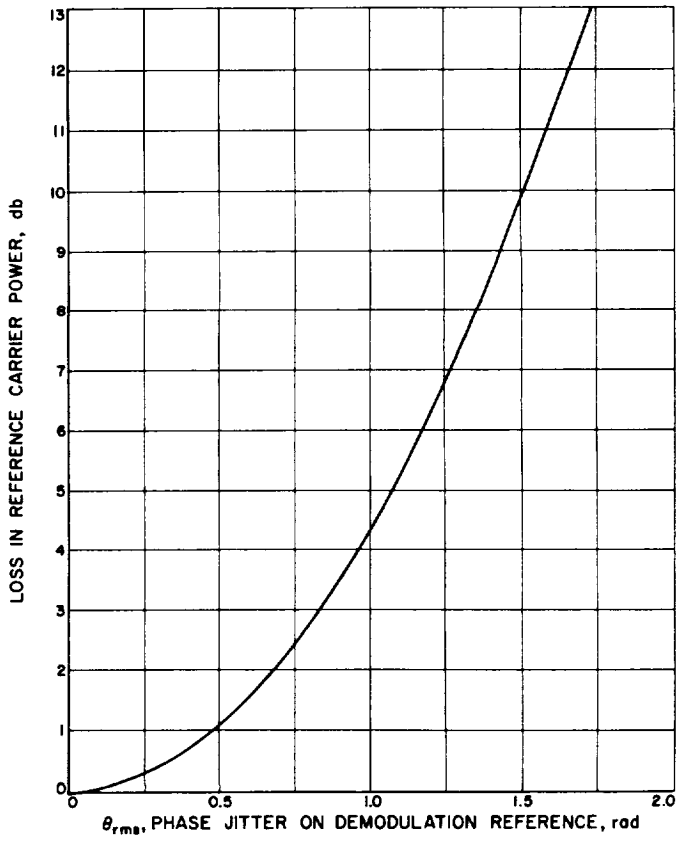

Fig. 21. Noisy demodulation reference SNR loss curve

same factor, or perhaps a combination of both. Since there is a lower limit on $2B_{Lo}$, owing to PN code acquisition time and the stability of the VCO itself, the resultant increase in synchronization power will become very significant at low data rates [and their low $S/(N/B)$ requirements] since the power must be diverted from the data channel, which means that the data rate must be correspondingly lowered to maintain the desired bit error probability.

These problems provided the motivation for the development of the Single-Channel Systems.

VI. SINGLE-CHANNEL SYSTEMS

A. Description of System

A near-optimum method of transmitting the data is to combine mod-2, the PN code, and the data. Thus, the output of the modulator would appear as $D \oplus \text{PN} \oplus 2f_s$ (D = data), which also may be represented by $\pm\text{PN} \oplus 2f_s$. A block diagram of the modulation system appears in Fig. 22. As can be seen, the data and synchronization are now embodied in a single signal or channel, and *all* of the available transmitter sideband power is allocated to it.

A problem now arises in the basic sync system detector when $\text{PN} \oplus 2f_s$ is modulated by the data. Referring back to Section IV, it is seen that the cross-correlation function shown in Fig. 10 is obtained for $+\text{PN} \oplus 2f_s$ correlated with PN, and therefore will be inverted for $-\text{PN} \oplus 2f_s$ correlated with PN. Obviously, such an occurrence cannot be tolerated, since the former state represents a stable PLL error function and the latter the unstable condition. As a result, the modulation of $\text{PN} \oplus 2f_s$ by the data must be removed prior to forming the PLL error function. Since no *a priori* knowledge of data is available within the detector, removal of the data component must be accomplished by means of cross-multiplication techniques.

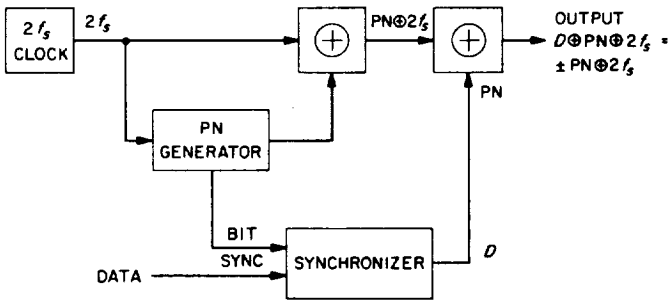

Fig. 22. Single-channel modulator

The properties of $\text{PN} \oplus 2f_s$, PN, and PN* readily lend themselves to the detector configuration shown in Fig. 23. The input signal, $\pm\text{PN} \oplus 2f_s$, is multiplied by both PN and PN* to obtain respectively $\pm 2f_s$ and $\pm f_s \angle 90$ deg when the PN components are correlated. The output of each multiplier is passed through a bandpass filter of appropriate center frequency and bandwidth to obtain data-modulated sine functions of $2f_s$ and $f_s \angle 90$ deg, which are then multiplied together to obtain a non-data-modulated waveform whose fundamental frequency is f_s. This signal, after filtering, is used to form the PLL error function through correlation with $f_s \angle 90$ deg.

The bandpass filters following the input multipliers are very significant to the system operation, and, in fact, the detector will not function properly without them. First, they are instrumental in forming the proper signal relationships, as without them, the output of the multiplier following them would be virtually independent of any detector inputs. Secondly, as will be shown later, they contribute to the formation of the PLL error function, and finally, their noise bandwidth is important in determining SNR losses that result in the multiplication of the noisy data-modulated $2f_s$ and $f_s \angle 90$ deg signals to obtain the non-phase-switching f_s component.

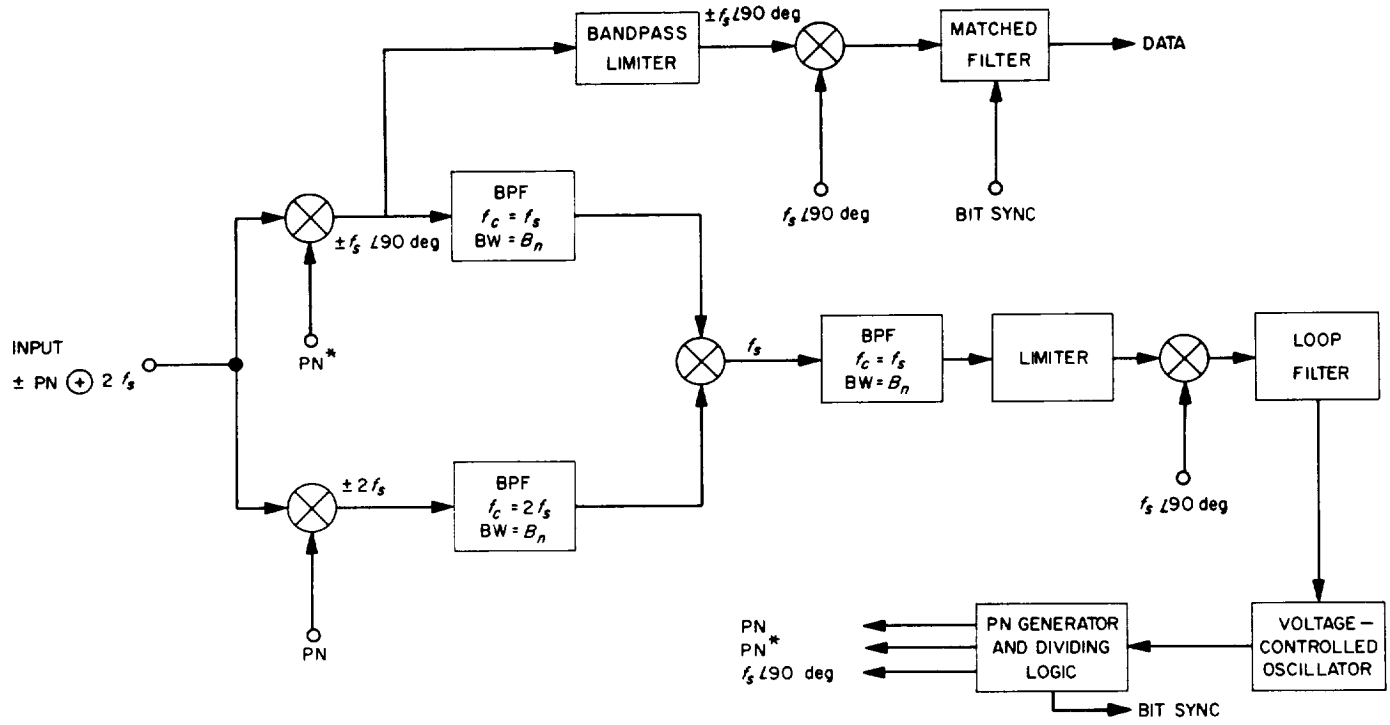

Fig. 23. Single-channel detector

The data-modulated signal $f_s\angle 90$ deg is passed through a bandpass limiter and is then multiplied by the coherent sync-loop $f_s\angle 90$ deg to recover the data in dc form. Note that the demodulation reference frequency is f_s rather than $4f_s$ as is the case in the two-channel systems, and the loss due to the noisy demodulation reference is significantly reduced. As in the two-channel system, an integrate-and-dump matched filter is then employed to optimize the decision process, with timing being supplied by the PN generator.

The foregoing system, which will be referred to as the Single-Channel System, possesses many of the desired properties set forth in Section II. Because all available transmitter sideband power resides in both the data and the synchronization signals, the requirement that synchronization should not degrade the system performance is met, and the synchronization signals will be as accurate and noise-free as possible. In addition, the mechanization of the detector is relatively simple and does not require extensive computer operations to acquire synchronization. The only apparent disadvantages of the system are the required transmission bandwidth and an $8/\pi^2$ loss in the data channel that results because $\pm f_s\angle 90$ deg is a square wave and only its fundamental is recovered. (If $\pm$PN* $\times$ $f_s\angle 90$ deg is used in place of $\pm \text{PN} \oplus 2f_s$, the $8/\pi^2$ loss will not result.)

B. PLL Error Signal

The PLL error signal in the Single-Channel System is somewhat altered from that obtained for the basic sync system, because of the data-modulation elimination circuit. In fact, if a careless comparison is made between the basic sync system and the complete single-channel detector with the data elimination circuit, the resulting single-channel error function seemingly does not exist. Put in other words, if a phase angle θ is introduced on the PLL reference f_s of the basic sync system, the loop error signal (tracing θ through the double loop) becomes a function of 2θ. However, when a phase angle of θ is introduced on the single-channel PLL reference, $f_s\angle 90$ deg, the loop error signal apparently does not reflect the phase error. Thus, the error signal for the single-channel PLL must be dependent not only upon the characteristics of the PN code but also upon the bandpass filters in the data elimination circuit.

In order to include the filters in the error function derivation, it is necessary to consider the Fourier coefficients at the output of the multipliers as a function of the PN code correlation coefficient τ. For simplicity, only the $2f_s$ and f_s components need be considered, since only they are instrumental in forming the loop error function.

The Fourier coefficients for a sine-cosine series representation of a time function $f(t)$ are given by

$$A_n = \frac{2}{T}\int_0^T f(t)\cos\left(\frac{2\pi nt}{T}\right)dt \tag{39}$$

and

$$B_n = \frac{2}{T}\int_0^T f(t)\sin\left(\frac{2\pi nt}{T}\right)dt \tag{40}$$

When $f(t)$ is a binary code and we are interested in multiples of f_s, Eqs. (39) and (40) become

$$A_k = 1/L \text{ Ave } \{\text{code} \oplus Kf_s\angle 90 \text{ deg}\} \tag{41}$$

$$B_k = 1/L \text{ Ave } \{\text{code} \oplus Kf_s\} \tag{42}$$

In the case under consideration, for $K = 1$ we have

$$\text{code} = \text{PN}\oplus 2f_s \oplus \text{PN}(\tau)\oplus f_s(\tau) \tag{43}$$

and for $K = 2$

$$\text{code} = \text{PN}\oplus 2f_s \oplus \text{PN}(\tau) \tag{44}$$

Thus,

$$A_1 = 1/L \text{ Ave } \{\text{PN}\oplus f_s \oplus \text{PN}(\tau)\oplus f_s(\tau)\} \tag{45}$$

$$B_1 = 1/L \text{ Ave } \{\text{PN}\oplus f_s\angle 90 \text{ deg}\oplus \text{PN}(\tau)\oplus f_s(\tau)\} \tag{46}$$

$$A_2 = 1/L \text{ Ave } \{\text{PN}\oplus 4f_s \oplus \text{PN}(\tau)\} \tag{47}$$

$$B_2 = 1/L \text{ Ave } \{\text{PN}\oplus \text{PN}(\tau)\} \tag{48}$$

Immediately, it can be recognized that A_1 and B_2 are respectively the PN* autocorrelation function and the PN autocorrelation function. The coefficients A_2 and B_1 also may be obtained readily through the methods employed earlier to derive the basic sync system error function.

The magnitude and phase for the filtered f_s and $2f_s$ signals are now evaluated through the relationships

$$\text{Magnitude} = \sqrt{A_k^2 + B_k^2} \tag{49}$$

$$\text{Phase} = \tan^{-1}(B_k/A_k) \tag{50}$$

and are plotted in Figs. 24 and 25. In making these plots, the values $n = 3$ and $L = 7$ were chosen, so that the slopes of the functions did not have to be derived in the rather cumbersome general forms.

The multiplication of $2f_s$ and f_s is now performed to obtain the f_s component (see Fig. 26), which in turn is multiplied by $f_s\angle 90$ deg, and the average taken to obtain the loop error function. A plot of the loop error function appears in Fig. 27. Note the very definite change in slope at $\pm 1/4$, indicating that the PLL changes bandwidth as a function of the position on the error curve. The ratio of the slopes is 4.7 and is directly related to the square of the PLL noise bandwidth; thus

$$2B_{L1}/2B_{L2} = 2.17 \tag{51}$$

The net effect of this phenomenon is that once the PN code is acquired, the loop bandwidth lowers (as long as operation is over the region of lower slope), thus reducing the amount of phase noise on the $f_s\angle 90$ deg reference, while during acquisition of the PN code, slightly higher drift rates are permitted.

C. Detector Performance

In order to relate the detector input SNR to the SNR at the input to the phase-locked loop, the SNR loss must be obtained for the multiplication of the noisy $2f_s$ and $f_s\angle 90$ deg signals. To derive a relationship, the following assumptions have been made:

1. The noise at the input to the system is Gaussian with a uniformly flat power spectral density over the frequency range of interest.

2. The effect of multiplying the input noise by either PN or PN* does not destroy its Gaussian character and only serves to translate, in frequency, its power spectral density.

3. When passing the noise through a bandpass filter, the output power spectral density of the noise will be rectangular and will occupy a bandwidth equal to the square or noise bandwidth, B_n, of the filter.

4. The noise bandwidths of the f_s and $2f_s$ filters do not overlap.

5. The presence of the data modulation has little, if any, effect on the final result, so that the $2f_s$ and $f_s\angle 90$ deg signals will be considered unmodulated.

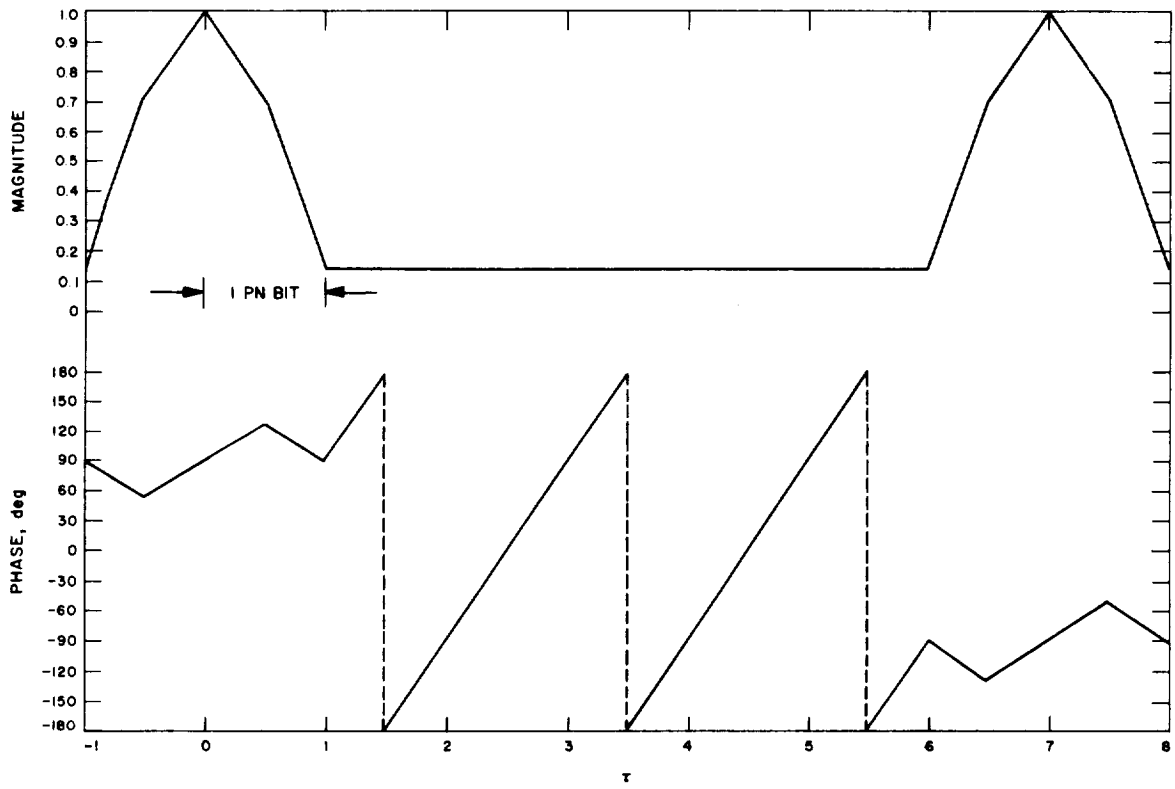

Fig. 24. Magnitude and phase of f_s

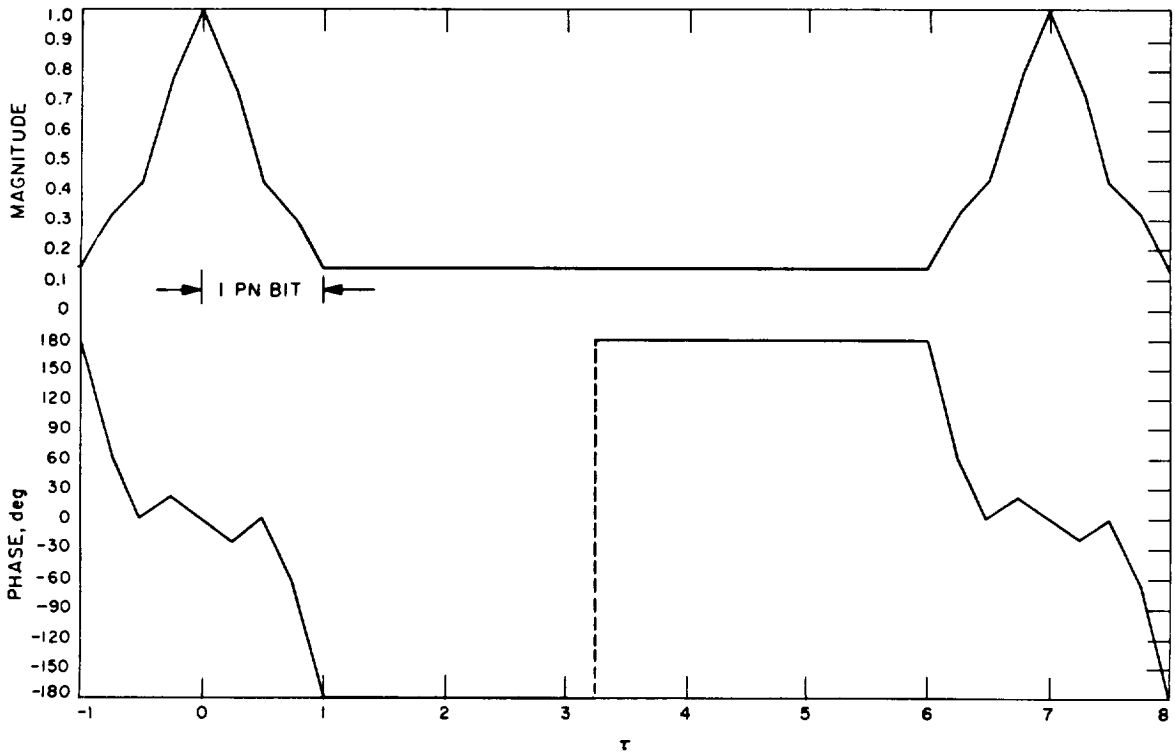

Fig. 25. Magnitude and phase of $2f_s$

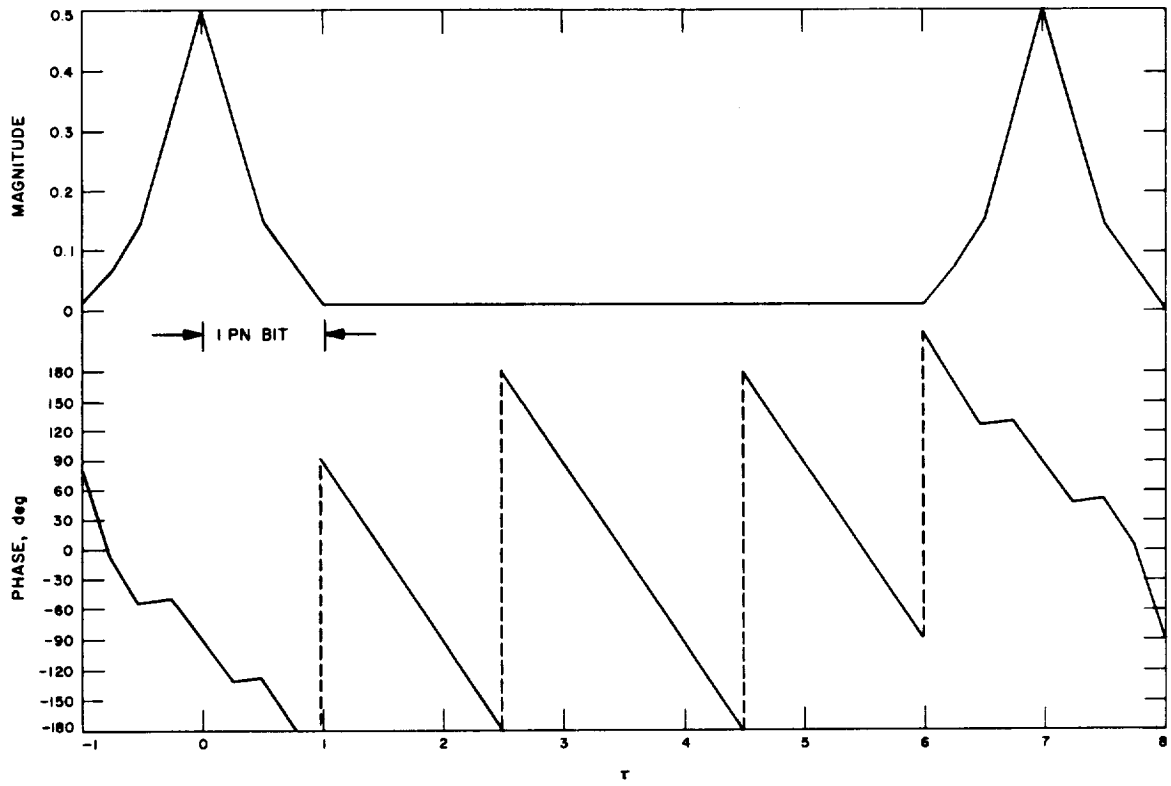

Fig. 26. Magnitude and phase of f_s input to PLL

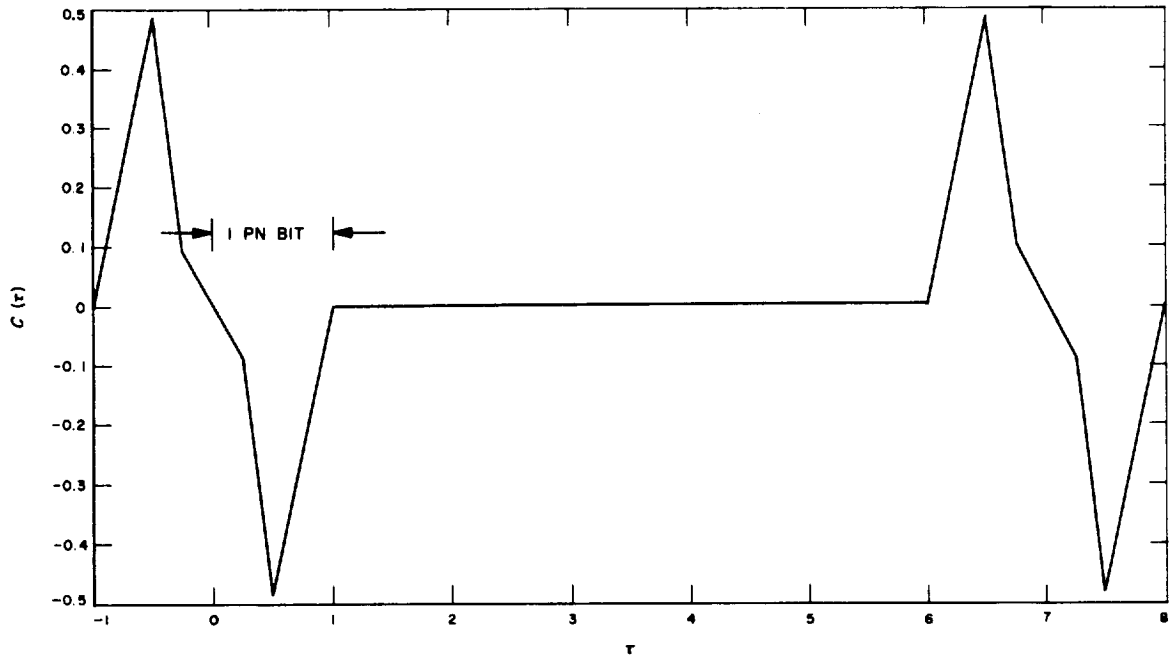

Fig. 27. Single-channel loop error signal

Multiplication of the input noise by PN and PN* results in two noise spectrums that are orthogonal or uncorrelated since

$$\text{Ave } \{PN \oplus PN^*\} = 0 \tag{52}$$

Thus, statistical dependence, like that found in square-law devices, need not be considered, and hence, the SNR at the output of the multiplier may be obtained through simple convolution of the signal and noise power spectral densities (Ref. 19).

At the output of the filters, the signals are $\sqrt{2}A \sin$, $(2\pi \cdot 2f_s t) + Kn_1(t)$ and $\sqrt{2}A \cos (2\pi \cdot f_s t) + Kn_2(t)$. The product yields

$$A^2 \sin (2\pi \cdot 3f_s t) + A^2 \sin (2\pi \cdot f_s t)$$

$$+ \sqrt{2}AKn_1(t) \cos (2\pi \cdot f_s t) \tag{53}$$

$$+ \sqrt{2}AKn_2(t) \sin (2\pi \cdot 2f_s t) + K^2 n_1(t) n_2(t)$$

The SNR output at f_s to the SNR input at $f_s \angle 90$ deg will be related. Thus, the SNR at the input is

$$(S/N)_{in} = (A^2/K^2)_{(BW=B_n)} \tag{54}$$

with the input noise bandwidth being B_n.

Performing the signal-on-noise and noise-on-noise convolutions for an output bandwidth equal to B_n, the sum of the noise voltage squared components is (see Fig. 28)

$$N^2_{out} = 3/8K^4 + A^2K^2 \tag{55}$$

and from Eq. (53) the output signal voltage squared is

$$S^2_{out} = A^4/2 \tag{56}$$

Taking the ratio of Eqs. (56) to (55) and relating terms to Eq. (54), the result is

$$(S/N)_{out} = \frac{(S/N)^2_{in}}{3/4 + 2(S/N)_{in}} \tag{57}$$

Figure 29 is a plot of this equation.

It can be seen from Eq. (57) that the minimum SNR loss is 3 db; i.e., for high-input SNR

$$(S/N)_{out} = 1/2(S/N)_{in} \tag{58}$$

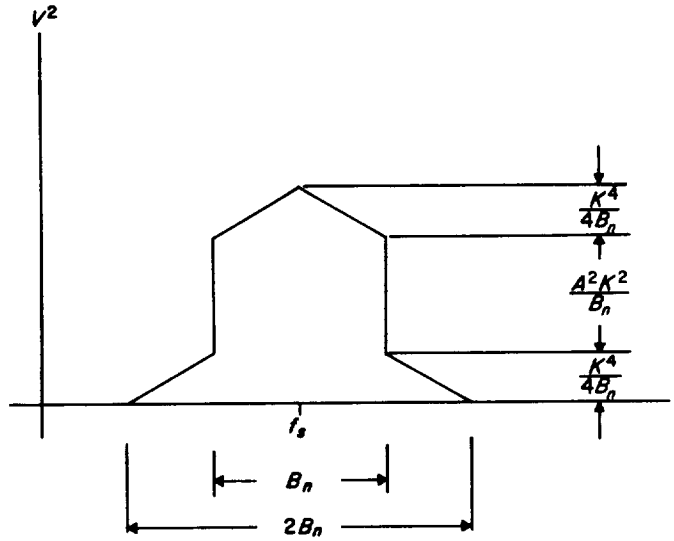

Fig. 28. Sum of noise voltage squared components

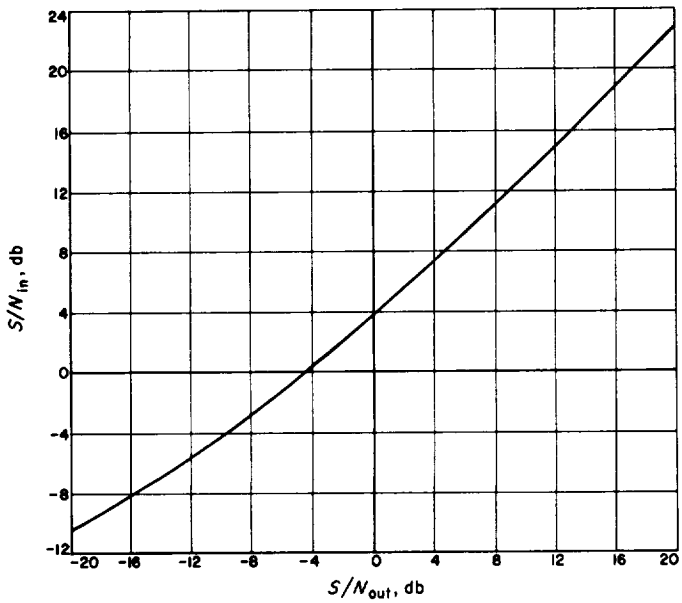

Fig. 29. Noisy multiplication SNR loss plot

At very low input SNR's, the output SNR varies as the square of input SNR, i.e.,

$$(S/N)_{out} = 4/3(S/N)^2_{in} \tag{59}$$

A more detailed examination shows that the input SNR to the multiplier should be kept above 4.0 db in order to hold the losses at a respectable level.

Equation (57) was derived assuming an ideal multiplier. In practice, near-ideal multipliers, such as the

should be as close to constant time delay as possible; otherwise, distortion of the loop error signal will result. By way of an example, consider the spectrum being recovered by means of a phase-lock receiver after being phase-modulated onto the RF carrier. The phase response between the loop signal input and the output of the phase detector is given by

$$\Phi = \tan^{-1} \frac{\sqrt{2}\omega/B_0}{(\alpha_0/\alpha)\left(\omega^2/B_0^2\right) - 1} \tag{64}$$

For $\omega >> B_0$, the linear approximation may be made such that

$$\Phi \approx \sqrt{2}(\alpha/\alpha_0)\,(B_0/\omega) \tag{65}$$

and the phase characteristics are linear. However, for

$$(\alpha_0/\alpha)\left(\omega^2/B_0^2\right) = 1$$

and less, the phase is very nonlinear. It has been found experimentally that if

$$0.394(\alpha_0/\alpha)\left(f_s^2/B_0^2\right) \geq 10 \tag{66}$$

no serious distortion will result. Note that the factor α_0/α is smallest when the RF system is considerably above threshold, indicating that the high-SNR condition represents the worst distortion condition. If the conditions of Eq. (66) cannot be met, then some suitable compensation network must be placed between the receiver and detector.

VII. FUTURE TRENDS

The single-channel system is being investigated for possible uses on advanced spacecraft during the latter portion of the 1960's and the early 1970's for both the telemetry and command links. The telemetry data rates will range between 5 and 5,000 bps, and command rates between 1 and 20 bps are contemplated.

The improvements that will be made in the single-channel system can only be conjectured at this point. Since the single-channel techniques make near-optimum use of the available transmitter sideband power, the next logical step would be to extend them directly into the RF domain so that splitting of the transmitter power between carrier and sidebands would no longer be required; in other words, the development of a suppressed carrier system. Methods have also been devised for combining relatively prime PN code lengths so as to form long codes with relatively short acquisition time for frame synchronization.

One possible future development might embody the functions of telemetry, command, and ranging (which also makes use of PN codes) into a single-coded two-way channel and thereby realize near-optimum use of the channel. In any event, the basic techniques will probably be with us for some time to come.

NOMENCLATURE

Abbreviations

bps	bits per second
DSIF	Deep Space Instrumentation Facility
MF	matched filter
PCM	pulse code modulation
PLL	phase-locked loop
PN	pseudonoise
PSK	phase-shift-keyed
SNR	signal-to-noise ratio
VCO	voltage-controlled oscillator

Symbols

B_0	natural frequency of loop, rad/sec
$2B_L$	loop noise bandwidth, cps
$2B_{L0}$	threshold loop noise bandwidth, cps
C	cross-correlation function
D	(1) antenna diameter, m (2) data
E	received signal energy per bit, joules
$erf(x)$	$\frac{2}{\sqrt{\pi}}\int_0^x e^{-t^2}dt$
f	transmitting frequency, Mc
f_s	PN code generator clock frequency, divided by two
$2f_s$	PN code generator clock frequency
$f_s \angle 90$ deg	PN code generator clock frequency, divided by two and phase-shifted 90 deg
G	parabolic antenna gain, db
G_R	receiving antenna gain, db
G_T	transmitting antenna gain, db
K	miscellaneous data channel losses
K_a	any miscellaneous loop gain or loss
K_M	multiplier constant, v/rad
K_{VCO}	VCO constant, rad/sec/v
L	length of periodic binary code
L_m	miscellaneous loss, db
L_S	free-space loss, db
L_T	system negative tolerances, db
N/B	noise power per unit bandwidth, w/cps
P_e^b	bit error rate or bit error probability
P_s	sideband transmitter power, dbm
R	(1) path distance, km (2) data rate, bps
$R(\tau)$	normalized time autocorrelation
$S(N/B)$	normalized received SNR, db-cps
T	bit period, sec
α	limiter signal voltage suppression factor
θ	rms phase jitter on the demodulation reference, rad
λ	limiter SNR factor
σ_n	rms phase jitter in phase-locked loop
τ	time displacement
Φ	normalized phase noise-to-signal ratio
Φ_K	receiving system noise spectral density, dbm/cps
$\oplus$	modulo-2 sum or mod-2 sum

REFERENCES

1. Riddle, F. M., "Communication With Deep Space Vehicles," *Proceedings of the 1962 National Telemetering Conference*, sponsored by the Institute of Radio Engineers, May 23–25, 1962, at Washington, D. C., Vol. I, p. 8–1.

2. Becker, H. D., and Lawton, J. G., *Theoretical Comparison of Binary Data Transmission Systems*, Cornell Aeronautical Laboratory Report No. CA-1172-S-1, May 1958.

REFERENCES (Cont'd)

3. Viterbi, A. J., *On Coded Phase-Coherent Communications*, Technical Report No. 32-25, Jet Propulsion Laboratory, Pasadena, California, August 1960.
4. Middleton, D., *An Introduction to Statistical Communication Theory*, McGraw-Hill Book Company, Inc., New York, 1960.
5. Baumert, L., Easterling, M., Golomb, S. W., and Viterbi, A. J., *Coding Theory and Its Applications to Communications Systems*, Technical Report No. 32-67, Jet Propulsion Laboratory, Pasadena, California, March 1961.
6. Golomb, S. W., *Sequences With the Cycle-And-Add Property*, Section Report No. 8-573, Jet Propulsion Laboratory, Pasadena, California, December 1957.
7. Peterson, W. W., *Error Correcting Codes*, The M.I.T. Press, Kendall Sq. Bldg., Cambridge 42, Mass., and John Wiley and Sons, Inc., New York, 1961.
8. Viterbi, A. J., "Phase-Lock-Loop Systems," in *Space Communications*, (A. V. Balakrishnan, ed.), McGraw-Hill Book Company, Inc., New York, 1963.
9. Jaffe, L., and Rechtin, E., "Design and Performance of Phase-Lock Circuits Capable of Near-Optimum Performance Over a Wide Range of Input Signal and Noise Levels," *IRE Transactions on Information Theory*, PGIT Vol. IT-1, No. 1, March 1955.
10. Martin, B. D., *The Pioneer IV Lunar Probe: A Minimum-Power FM/PM System Design*, Technical Report No. 32-215, Jet Propulsion Laboratory, Pasadena, California, March 1962.
11. Viterbi, A. J., *Acquisition and Tracking Behavior of Phase-Locked Loops*, External Publication No. 673, Jet Propulsion Laboratory, Pasadena, California, July 1959.
12. Gilchriest, C. E., "Application of the Phase-Locked Loop to Telemetry as a Discriminator or Tracking Filter," *IRE Transactions on Telemetry and Remote Control*, Vol. TRC-4, No. 1, June 1958.
13. Davenport, W. B., Jr., "Signal-to-Noise Ratios in Band-Pass Limiters," *Journal of Applied Physics, Vol. 24, No. 6*, June 1953.
14. Rowbotham, J. R., *Phase-Locked Loop Study*, Phase I of Project 2-520-1202, Motorola Inc., Military Electronics Division, June 1961.
15. Gilchriest, C. E., *Research Summary No. 36-9*, Vol. 1, Jet Propulsion Laboratory, Pasadena, California, July 1961, p. 51.
16. Titsworth, R. C., and Welch, L. R., *Power Spectra of Signals Modulated by Random and Pseudorandom Sequences*, Technical Report No. 32-140, Jet Propulsion Laboratory, Pasadena, California, October 1961.
17. Bryden, J. N., *Mariner (Venus '62) Flight Telecommunication System*, Technical Report No. 32-377, Jet Propulsion Laboratory, Pasadena, California, January 15, 1963.
18. Gilchriest, C. E., *Space Programs Summary No. 37-16*, Vol. IV, Jet Propulsion Laboratory, Pasadena, California, August 31, 1962, p. 87.
19. Davenport, W. B., Jr., and Root, W. L., *Random Signals and Noise*, McGraw-Hill Book Company, Inc., New York, 1958.